Dyes and Pigments 163 (2019) 454–474

Contents lists available at ScienceDirect

Dyes and Pigments

journal homepage: www.elsevier.com/locate/dyepig

Investigating Asian colourants in Chinese textiles from Dunhuang (7th-10th century AD) by high performance liquid chromatography tandem mass spectrometry – Towards the creation of a mass spectra database

Diego Tamburini

Department of Scientific Research, The British Museum, Great Russell Street, London, WC1B 3DG, UK

ARTICLE INFO

Keywords:
HPLC-MS
Tandem mass spectra
Asian dyes
Chinese textiles
Dunhuang
Silk Road

ABSTRACT

A broad palette of natural dyes is often mentioned with reference to dyed textiles from ancient China. However, few scientific works address the problem of correctly identifying these dyes, often referring simply to unidentified sources.

The aim of this work was the creation of a database of mass spectra of molecules related to Chinese natural dyes, intended to be used for their identification in archaeological textiles. High pressure liquid chromatography coupled with electrospray ionisation and quadrupole time-of-flight detection (HPLC-ESI-Q-ToF) was used to analyse twenty-eight reference specimens of Asian dyes, including relatively common dyes, such as sappanwood (*Biancaea sappan*), gromwell (*Lithospermum erythrorhyzon*), safflower (*Carthamus tinctorius*), madder (*Rubia tinctorum*, *Rubia cordifolia* and *Rubia akane*), and unusual dyes, such as rosewood (*Dalbergia* sp.), rhubarb (*Rheum emodi*), dragon's blood (*Daemonorops* sp.), gamboge (*Garcinia hanburyi*), violet (*Viola yedoensis*), *etc*. All analyses were repeated after artificial ageing, thus showing which molecules are more likely to be considered as markers for the identification of these dyes in ancient textiles. Because of the dye sources chosen, most molecular classes of natural organic colourants were included in the mass spectra database, *i.e.* anthraquinones, naphthoquinones, flavonoids, neoflavonoids, alkaloids, chalcones, carotenoids, xanthenes, polyphenols, *etc*. The information obtained from the reference specimens was then used to identify the dyes in thirty-one textiles from Dunhuang (northwestern Gansu, China, 7th-10th century AD) in the British Museum's collection. The sampling was guided by the data previously gathered from multispectral imaging and fibre optic reflectance spectroscopy (FORS), presented in a separate paper. Mixtures of dyes were commonly found, leading to hypothesise the re-dyeing or recycling of some of the textiles. A very broad palette of dyes suggested possible different origins for these textiles and a tendency to experiment with dyeing. These data, integrated with the ones obtained non-invasively, represent a significant source of information for researchers investigating textiles from the Silk Road.

1. Introduction

For various reasons, the identification of natural dyes in archaeological textiles is a challenging task from a scientific point of view. The geographical variability of dye sources makes the identification strictly dependant on the availability of reference materials, which are sometimes not easily accessible [1]. Moreover, the ageing of the textiles and the degradation of the dye molecules generally produce colour change, differences in the photophysical properties and a reduction/change of the molecular markers that can be used for identification [2–4]. Finally, the level of information and the probability of identification vary according to the investigative approach chosen [5].

Generally, dye molecules belong to a broad range of molecular categories, such as anthraquinones, flavonoids, neoflavonoids, indigoids, carotenoids, chalcones, alkaloids, xanthones, naphthoquinones, anthocyanins, tannins, *etc*. Such variety of chemical structures requires robust analytical methodologies able to provide reliable responses for all these classes of molecules [5–11]. Sometimes textiles are considered too precious or too fragile to allow sampling. Non-invasive techniques, such as fluorescence spectroscopy [12,13], UV–Vis reflectance spectroscopy [14] and multispectral imaging [15,16], and micro-invasive techniques, such as SERS [17], have shown their potential for dye identification when access for sampling is restricted. However, some dye molecules do not produce signals specific enough to enable their identification non-invasively, especially most yellow dyes [12,18]. Sampling opens the possibility of obtaining information that relates more deeply to the molecular structure of the dye molecules. Having access to the exact molecular composition of a sample is the only way dye sources can be

E-mail address: DTamburini@britishmuseum.org.

https://doi.org/10.1016/j.dyepig.2018.12.025
Received 5 November 2018; Received in revised form 14 December 2018; Accepted 14 December 2018
Available online 16 December 2018
0143-7208/

Fig. 1. Image of the set of reference samples under investigation. The samples are shown as pairs: for each pair the upper samples are non-aged and the lower samples are aged. In the low part of the image, the samples on the left are non-aged and the samples on the right, representing a sub-sample of the samples from the left, are aged.

identified with extreme precision, down to the exact plant or animal species. Nowadays, HPLC-MS is the technique of choice for obtaining such information, and the amount of sample needed is generally very small (2–3 mm of a thread) [6,10,19], which usually makes the small damage on the textile acceptable considering the level of information gained. However, due to the high number of molecular classes potentially present in a sample, extraction procedures and detection conditions must be optimised, in order not to discriminate certain categories of molecules over others [8,20,21]. Extraction procedures combining different solvents and mild acidic conditions appear to be the most suitable for this task and also to ensure the preservation of the molecular structures without alteration, for example avoiding the cleavage of the glycosidic bonds in dyes containing conjugated flavonoids [2,22–27].

This paper presents the results obtained by HPLC-MS for the identification of the dyes in thirty-one textiles from Dunhuang (northwestern Gansu, China) dating from the 7th to the 10th century AD. Before taking a limited number of samples, these textiles were investigated non-invasively, using digital microscopy, multispectral imaging and fibre optic reflectance spectroscopy (FORS) [16]. To achieve the identification, a set of reference samples was created by dyeing silk fabrics with twenty-eight sources of dyes mostly mentioned in historical manuscripts [27–29].

Previous works have addressed the identification of Asian dyes adopting different approaches [18,20,30–40] and a few studies focusing on mass spectrometric data are available [22,27,35,41–43].

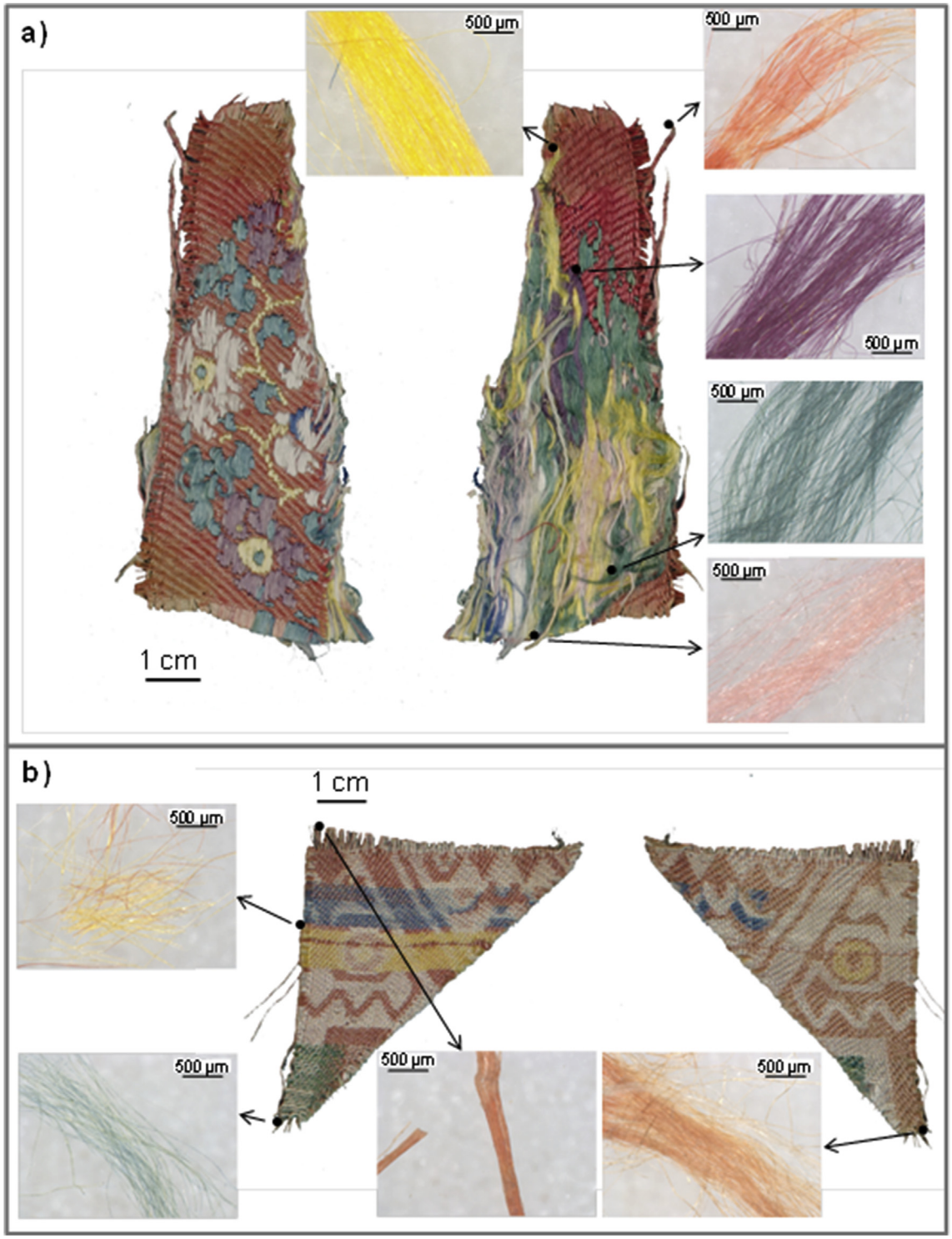

Fig. 2. Images of the front and the back of the textiles MAS.871 (a) and MAS.872 (b) showing the sampling positions and micrographs of the samples recorded with an optical microscope.

Nevertheless, the literature is very fragmentary on this topic and most of the research done supports single case studies. This study represents the most systematic work undertaken on the topic and includes the most complete collection of data. In addition, the archaeological complex of Dunhuang, which is considered a pearl amongst discoveries on the Silk Road, is of paramount importance in the field of oriental studies. The caves had been sealed from the beginning of the 11th century until their discovery in the early 1900s [44]. The extremely dry environmental conditions permitted the exceptional preservation of the works of art present in the caves, not only colourful mural paintings and statues, but also organic materials, such as documents, silk paintings and textiles, whose production spanned from the 6th to the 11th century [45,46]. Although the mural paintings probably attracted the highest level of attention and the greatest number of studies, the textiles were equally impressive. They consisted of canopies, banners, sutra covers and wrappers, polychrome and monochrome woven silk, clamp-resist dyed silk and embroidered silk [44].

It was Sir Aurel Stein who acquired many objects, including a large

Table 1
List of the textiles analysed, samples taken and main results obtained by HPLC-MS. The information obtained non-invasively is also reported for comparison.

Object Number	Samples	HPLC-MS results	Markers detected	FORS and MSI results [16]
Monochrome woven silk textiles				
MAS.890	yellow	smoketree and pagoda tree	sulfuretin, butin and butein, fustin, rutin	unidentified
MAS.935	yellow	Chinese cork tree	berberine, jatrorrhizine, hydroxyberberine	protoberberine-based
MAS.936	yellow	safflower and Chinese cork tree	carthamin, carthamin degradation products (*m/z* 449 and 477), *m/z* 582, apigenin, berberine (traces)	protoberberine-based (probably low concentration)
MAS.938	yellow	safflower	carthamin, carthamin degradation products (*m/z* 449 and 477), *m/z* 582	faded safflower and unidentified yellow
MAS.942	yellow	pagoda tree	rutin	unidentified
MAS.904	orange	safflower	carthamin, carthamin degradation products (*m/z* 449 and 477), *m/z* 582	safflower
MAS.951	orange	safflower	same as MAS.904	safflower
MAS.939	red	dyer's madder	alizarin (high), munjistin, purpurin, pseudopurpurin, rubiadin, ruberythric acid, lucidin primveroside	unidentified
MAS.954	red	Indian madder and sappanwood	munjistin, purpurin, pseudopurpurin, rubiadin (high), rubiadin primveroside, urolithin C	plant-based red, probably madder
MAS.896	brown	madder, sappanwood and gromwell	rubiadin, urolithin C, shikonin, *m/z* 205 and 259	gromwell
MAS.949	brown	gromwell and lac dye	*m/z* 205 and 259, aleuritic acid, jalaric-aleuritic ester	gromwell
MAS.891	purple	dyer's madder and gromwell	alizarin, munjistin, pseudopurpurin (high), purpurin (high), rubiadin, ruberythric acid, lucidin primveroside; shikonin, *m/z* 205, 259 and 285	gromwell
MAS.900	purple	dyer's madder and gromwell	same as MAS.891	gromwell
MAS.901	purple	dyer's madder and gromwell	same as MAS.891	gromwell
MAS.902	purple	dyer's madder and gromwell	same as MAS.891	gromwell
MAS.903	purple	dyer's madder and gromwell	same as MAS.891	gromwell
MAS.937	purple	dyer's madder and gromwell	same as MAS.891	gromwell
Polychrome woven silk textiles				
MAS.865	orange	sappanwood	urolithin C, brasilin, brasilein, sappanol, protosappanin B, D and E	safflower (?)
	red	sappanwood	urolithin C, brasilin, brasilein, sappanol, protosappanin B, D and E	safflower (?)
	yellow	unidentified	luteolin glucoside, isoquercitrin, *m/z* 433 ($C_{21}H_{22}O_{10}$) and *m/z* 449 ($C_{21}H_{22}O_{11}$)	unidentified
MAS.869	yellow	pagoda tree	rutin, isorhamentin rutinoside	unidentified
	green	pagoda tree and indigo	rutin, isorhamentin rutinoside, isatin, indigotin, indirubin	unidentified yellow and indigo
	purple	gromwell	shikonin, emodin *m/z* 205, 259, 285	gromwell
MAS.871	red	safflower	carthamin, carthamin degradation products (*m/z* 449 and 477), *m/z* 582	safflower
	purple	gromwell and sappanwood	shikonin, *m/z* 205, 259, 285, urolithin C, brasilin	gromwell
	yellow	pagoda tree	rutin, isorhamentin rutinoside	unidentified
	green	pagoda tree and indigo	rutin, isorhamentin rutinoside, isatin, indigotin, indirubin	unidentified yellow and indigo
	pink	safflower	carthamin, carthamin degradation products (*m/z* 449 and 477), *m/z* 582	safflower
MAS.872	yellow	larkspur	kaempferol-3-*O*-glucoside, quercetin-3-*O*-glucoside, isorhamnetin-3-*O*-glucoside	unidentified (carotenoid?)
	green	larkspur and indigo	kaempferol-3-*O*-glucoside, quercetin-3-*O*-glucoside, isorhamnetin-3-O-glucoside, isatin, indigotin, indirubin	unidentified yellow and indigo
	red	sappanwood	urolithin C, brasilin	sappanwood (?)
	red back	sappanwood	urolithin C, brasilin	sappanwood (?)
MAS.873	yellow	unidentified	same as MAS.865_yellow	unidentified
	green	larkspur and indigo	kaempferol-3-*O*-glucoside, quercetin-3-*O*-glucoside, isorhamnetin-3-*O*-glucoside, isatin, indigotin, indirubin	unidentified yellow and indigo
	orange	sappanwood and unidentified yellow	same as MAS.865_yellow, urolithin C, brasilin	safflower (?)
MAS.906.a-b	yellow	pagoda tree	rutin, isorhamentin rutinoside	unidentified
	green	desert poplar or *Vitex negundo* + indigo	luteolin-7-*O*-glucoside, luteolin-8-*C*-glucoside, apigenin-7-*O*-glucuronide, luteolin-7-*O*-glucuronide, *C*-glucoside with *m/z* 475, luteolin, isatin, indigotin, indirubin	unidentified yellow and indigo
MAS.908.a-b	pink	sappanwood	urolithin C	unidentified
	yellow	Chinese cork tree	berberine, methylberberine, hydroxyberberine	protoberberine-based
MAS.920	yellow	weld	apigenin, luteolin, chrysoeriol, luteolin oxidation products	unidentified
MAS.922	red	sappanwood	urolithin C, brasilin, brasilein, sappanol, protosappanin D and E	sappanwood (?)
	yellow	saffron	kaempferol-*O*-glucoside, *m/z* 533, crocin B, crocin C, crocin B (formic acid adduct), crocin C (formic acid adduct)	unidentified
MAS.924	yellow	pagoda tree and sappanwood	rutin, isorhamentin rutinoside, urolithin C	unidentified
	green	desert poplar or *Vitex negundo* and indigo	luteolin-7-*O*-glucoside, luteolin-8-*C*-glucoside, apigenin-7-*O*-glucuronide, luteolin-7-*O*-glucuronide, *C*-glucoside with *m/z* 475, luteolin, isatin, indigotin, indirubin	unidentified yellow and indigo
	beige	sappanwood and smoketree	urolithin C, fisetin	unidentified

(*continued on next page*)

Table 1 (*continued*)

Object Number	Samples	HPLC-MS results	Markers detected	FORS and MSI results [16]
MAS.929	yellow	safflower and cape jasmine	carthamin, carthamin degradation products (*m/z* 449 and 477), *m/z* 582, geniposide (formic acid adduct), *m/z* 533, 5-*O*-caffeoyl-4-*O*-sinapoylquinic acid, crocin C, 3,5-di-*O*-caffeoyl-4-*O*-(3-hydroxy-3-methyl)-glutaroylquinic acid, crocin C (formic acid adduct), crocin A	unidentified
	black	Chinese sumac (?)	ellagic acid	tannins
Embroidered silk textiles				
MAS.911	brown (ground)	dyer's madder and condensed tannins	alizarin, munjistin, pseudopurpurin, purpurin, rubiadin, nordamnacanthal, ruberythric acid; ellagic acid; cluster *m/z* 700-800	plant-based red (madder) and tannins (?)
MAS.915	red	dyer's madder	alizarin (high), munjistin, pseudopurpurin, purpurin, rubiadin, nordamnacanthal, ruberythric acid	plant-based red, probably madder
	light green	Japanese barberry and indigo	berberine, palmatine, jatrorrhizine (high) dihydropalmatine, *m/z* 298, 305, isatin, indigotin, indirubin	protoberberine-based yellow and indigo
	dark green	Japanese barberry and indigo	berberine, palmatine, jatrorrhizine (high), dihydropalmatine, *m/z* 298, 305, isatin, indigotin, indirubin	protoberberine-based yellow and indigo
MAS.1130	yellow 1	Chinese cork tree	berberine, methylberberine, hydroxyberberine, jatrorrhizine	protoberberine-based yellow
	yellow 2	Chinese cork tree	berberine, methylberberine, hydroxyberberine, jatrorrhizine	protoberberine-based yellow
	light yellow	not detected		unidentified
	dark green	desert poplar or *Vitex negundo*, Chinese cork tree and indigo	luteolin-7-*O*-glucoside, luteolin-8-*C*-glucoside, luteolin-7-*O*-glucuronide, *C*-glucoside with *m/z* 475, berberine, hydroxyberberine, jatrorrhizine, isatin, indigotin, indirubin	unidentified yellow and indigo
	green	Chinese cork tree and indigo	berberine, methylberberine, hydroxyberberine, jatrorrhizine, isatin, indigotin, indirubin	unidentified yellow and indigo
	brown/red	Indian madder and unidentified	alizarin (very low), munjistin (high), pseudopurpurin, purpurin, rubiadin, kaempferol, quercitrin	plant-based red (probably madder) and tannins
	red	Indian madder	alizarin (very low), munjistin (high), pseudopurpurin, purpurin, rubiadin	plant-based red, probably madder
	pink	lac dye	laccaic acids A, B, C, E, *m/z* 634, rubiadin	insect-based red
	purple	Indian madder and indigo	alizarin (very low), munjistin (high), pseudopurpurin, purpurin, rubiadin isatin, indigotin, indirubin	plant-based red (probably madder) and indigo

number of textiles and textile fragments, and brought them to Britain in the early 1900s [47]. In London these textiles are now divided among the collections of the British Museum, the Victoria and Albert Museum and the British Library, but Dunhuang textiles are spread all over the world in the collections of many major museums [44,48,49]. Generally, the textiles have been catalogued and studied from a technical point of view. In addition, some knowledge is available about textile production and dyeing practices in ancient China [1]. However, most information refers to later periods, such as Ming (1368–1644 AD) and Qing (1644–1911 AD) dynasties [28].

For all these reasons, the results shown in this paper represent valuable information with a broad interest for the scientific and museum communities, providing a significant advancement for the identification of Asian dyes by HPLC-MS and for the knowledge of Dunhuang textiles.

2. Materials and methods

2.1. Reference material

Twenty-eight specimens of raw materials were collected from different sources. These included *Phyllanthus emblica* (Indian gooseberry), *Rhus* sp. (Chinese sumac), *Juglans regia* (walnut tree), *Rubia cordifolia* (Indian madder, munjeet), *Rubia tinctorum* (dyer's madder), *Rubia akane* (Japanese madder), *Kerria lacca* (Indian lac dye), *Biancaea sappan* (sappanwood), *Pterocarpus santalinus* (sandalwood), *Carthamus tinctorius* (safflower), *Lithospermum erythrorhizon* (gromwell), *Rheum emodi* (rhubarb), *Dalbergia* sp. (rosewood), *Daemonorops* sp. (dragon's blood), *Curcuma longa* (turmeric), *Gardenia jasminoides* (cape jasmine), *Crocus sativus* (saffron), *Phellodendron amurense* (amur-cork tree), *Coptis chinensis* (Chinese goldthread), *Berberis thunbergii* (Japanese barberry), *Symplocos* sp. (Lodh tree/Asiatic sweetleaf), *Viola yedoensis* (violet), *Sophora japonica* (pagoda bud), *Rhamnus saxatilis* (buckthorn), *Garcinia hanburyi* (gamboge), *Reseda luteola* (weld), *Miscanthus sinensis* (silver grass) and *Cotinus coggygria* (smoketree).

These dye sources were chosen on the basis of available literature on natural Asian dyes potentially available in Tang dynasty China [1,3,28,29,31,34,35,42] and were used to create a reference set of dyed silk samples. The details about the acquisition of the dyes, the preparation of the samples, including the parts of the plants used and the dyeing processes, are presented in Ref. [16]. An image of the samples obtained before and after ageing is shown in Fig. 1.

2.2. Archaeological textiles and samples

Seventeen monochrome woven silk, eleven polychrome woven silk and three embroidered silk textiles were chosen from the Stein collection in the British Museum. The textiles, mainly fragments, are dated from the late 7th to the early 10th century (Tang to Five Dynasties period) and represent various weaving techniques (damask, gauze, brocade, samite, *etc.*). They show a wide range of colour shades, including yellow, orange, pink, red, brown, purple, green and blue.

The textiles were investigated non-invasively using digital microscopy (DM), multi-spectral imaging (MSI) and fibre optic reflectance spectroscopy (FORS), and some information about the dyes present was obtained as described in Ref. [16] and was used to guide the sampling. One sample was then taken from each monochrome textile fragment and a selection of sampling areas was identified for each polychrome and embroidered textile. In most cases, samples were taken from the back of textiles, by selecting loose threads. The focus was on yellow, red, orange, pink and purple colours. The blues were excluded from the invasive investigation, as the presence of indigo was clear from MSI and FORS results and additional information about the exact source of the dye cannot be obtained chemically.

A description of the textiles is provided in Ref. [16]. Fig. 2 shows two of the textiles with the sampling areas indicated and micrographs of the samples taken. Images of the other textiles and corresponding samples are reported in the Supplementary Information (Figs. S1–12). Table 1 reports the number of samples taken from each textile and a summary of results obtained by HPLC-ESI-Q-ToF for all the textiles analysed. A summary of the information obtained by the non-invasive analyses [16] is also provided for comparison.

2.3. Artificial ageing

Artificial ageing was performed on the set of reference samples in order to evaluate changes in the chemical composition induced by an accelerated ageing/fading simulating the results of a long-time exposure in a museum environment. An Atlas SolarClimatic SC 340 MH climatic chamber was used. This was equipped with a metal halide lamp simulating solar radiation and a UV filter (5 mm LEXAN filter with a Sun-X MT20 film) to cut the radiation below 400 nm and reduce the total light to 0.027 Mlux h^{-1}. The temperature was set at 40 °C and relative humidity was set to 50%. The experiment lasted four weeks (672 h) and the samples were exposed to *ca.* 18.15 Mlux. Further details about the conditions of the ageing are described in Ref. [16].

2.4. Optical microscopy (OM)

Examination by optical microscopy was carried out on the samples using a Leica MZ6 stereomicroscope equipped with a ScopeTeck DCM900 digital camera.

2.5. HPLC-ESI-Q-ToF

The reference samples were analysed before and after ageing. For these samples *ca.* 5 mm (*ca.* 150 μg) of a single thread were used. These are usually considered large samples, as a successful analysis can generally be done with half of this amount. In fact, for the Dunhuang samples, 2–3 mm (*ca.* 100 μg) of single threads were taken.

All the samples were treated using the method published in Ref. [22], which briefly consists of a double mild extraction procedure using DMSO and a mixture of methanol/acetone/water/0.5M oxalic acid 30:30:40:1 (v/v/v/v). The method has proven suitable for the analysis of organic colourants in both dyes [15,22,27] and pigments formulations [50,51].

Analyses were carried out using a 1260 Infinity HPLC (Agilent Technologies), coupled to a Quadrupole-Time of Flight tandem mass spectrometer 6530 Infinity Q-ToF detector (Agilent Technologies) by a Jet Stream ESI interface (Agilent Technologies). Separation was achieved using a Zorbax Extend-C18 column (2.1 mm × 50 mm, 1.8 μm particle size) with a 0.4 mL/min flow rate and 40 °C column temperature, and a gradient of water with 0.1% formic acid (eluent A) and acetonitrile with 0.1% formic acid (eluent B). The elution gradient was programmed as follows: initial conditions 95% A, followed by a linear gradient to 100% B in 10 min, and held for 2 min. Re-equilibration time for each analysis was 10 min. 5 μL injection volume was adopted for MS experiments and 10 μL for MS/MS experiments.

The ESI operating conditions were: drying gas (N_2, purity > 98%) temperature 350 °C and 10 L/min flow; capillary voltage 4.0 kV; nebulizer gas pressure 40 psig; sheath gas (N_2, purity > 98%) temperature 375 °C and flow 11 L/min.

High resolution MS and MS/MS spectra were acquired in positive and negative mode in the range 100–1700 *m/z*. The fragmentor was kept at 150 V, nozzle voltage 1000 V, skimmer 65 V, octapole RF 750 V. For the MS/MS experiments, different voltages (from 10 to 40 V) in the collision cell were tested for Collision Induced Dissociation (CID), in order to maximise the information obtained from the fragmentation. The collision gas was nitrogen (purity 99.999%). The data were collected by targeted MS/MS acquisition with an MS scan rate of 1.0 spectra/sec and a MS/MS scan rate of 1.0 spectra/sec. Auto-calibration was performed daily using Agilent tuning mix HP0321 (Agilent Technologies) prepared in 90% water-10% acetonitrile.

MassHunter® Workstation Software was used to carry out mass spectrometer control, data acquisition, and data analysis. In particular, extract ion chromatograms were obtained using the software EIC function and selecting the mass range corresponding to the calculated mass ± 0.001 *m/z*.

3. Results

3.1. Reference samples

The chromatographic profiles obtained from most of the reference samples were very complex, showing a high number of molecules. The identification of these molecules was based on the accurate masses of their protonated $[M+H]^+$ or deprotonated ions $[M-H]^-$ and their fragmentation spectra. The instrumental accuracy in mass measurements resulted in a difference between the experimental accurate masses and the calculated masses below 2 ppm in all cases. Considering that 2 ppm of 500 *m/z* corresponds to 0.001 *m/z* and that the molecules considered in this work are in the approximate range of 250–900 *m/z*, mass values are here reported with three decimal digits. In the case of molecules present in the in-house database, retention times were also used to compare with the standard molecules. MS/MS data available in the literature were used in the majority of the cases where a standard molecule was not available for direct comparison. Some tentative assignments were made by interpreting the tandem mass spectra of unknown molecules. The main molecules present in each reference sample are listed in Table S1 (Supplementary Information), together with their mass spectrometric details. Some of the molecules are evidenced and referred to as markers of identification of a specific dye source. The criteria used to define these markers were i) for the molecules to be present after artificial ageing and ii) for the molecules not to be ubiquitous, *i.e.* present in many samples. Figs. 3 and 4 show the molecular structures and *m/z* of the molecular ions of most of these marker molecules, highlighting the variety of molecular classes to which they belong.

During the discussion of the results, the relative abundance of compounds is sometimes mentioned in this paper. It is important to underline that this refers to the chromatographic peak areas (as obtained from the extract ion chromatograms – see section 2.5), which are a result of both the concentration and the ionisation yield of molecules. As no calibration curve has been performed in this study, the relative abundance of the peaks is not directly related to the actual concentration of the molecules in the samples. However, as the same analytical conditions were applied to all samples, internal comparisons within the dataset are scientifically acceptable, for example between non-aged and aged samples.

3.1.1. Brown

The brown samples (Indian gooseberry, walnut and Chinese sumac) had very different compositions. Indian gooseberry (*P. emblica*) fruits are reported to be a rich source of (poly)phenolic compounds, such as flavonoids and hydrolysable tannins. Gallic acid, ellagic acid, corilagin, chebulagic acid, quercetin and kaempferol are mentioned as the main components in the extracts of various parts of the plant [52,53], and a high number of minor compounds are also reported [54,55]. In these analyses ellagic acid, kaempferol, quercetin and quercetin glycosides (quercitrin - quercetin-3-*O*-rhamnoside - and rutin - quercetin-3-*O*-rutinoside) were detected in the non-aged sample, suggesting that these are the molecules with the highest affinity for the silk fibres. However, after ageing, the main compounds detected in the sample were hydroxybenzoic acids (3,4-dihydroxybenzoic and 4-hydroxybenzoic acids), which are known to be degradation products of tannins and flavonoids [56].

Walnut husks (*J. regia*) are also known to contain phenolic acids, flavonoids and tannins, but, among them, juglone (5-hydroxy-1,4-napthoquinone) is unique to walnuts [57] and can be used as marker to identify the walnut tree as a source of brown colour [1]. In the case of these analyses, juglone ($[M-H]^-$ = 173.024 *m/z*) was detected together with luteolin, quercetin, quercetin-3-O-glucoside, quercitrin, juglanin B and juglanin C [58], as well as an unknown compound with *m/z* 189.019. The mass of the deprotonated ion $[M-H]^-$, as well as the tandem mass spectrum, suggested the presence of an additional oxygen atom on the juglone molecule. Therefore, this compound was tentatively assigned to the hydroxyl or oxo-juglone.

The results obtained for the Chinese sumac (*Rhus* sp.) sample were in agreement with the high content of hydrolysable tannins generally present in the *Rhus* plants [1,59,60]. The exact species of this specimen could not be identified, despite the use of SEM to investigate the wood anatomical features, although the genus was confirmed as *Rhus*. However, different *Rhus* species are commonly referred to as Chinese sumac in the literature [1,29] and the exact identification was not necessary for the purposes of this work. Ellagic acid, 3,4,5–trihydroxy-2-oxo-1,3-propanediyl ester of benzoic acid, tetragalloyl-glucoside and various other glucosides of ellagic and gallic acids were identified. Just a slight increase in the relative abundance of ellagic acid was detected after ageing and the rest of the profile was very similar, highlighting a certain degree of hydrolysis but also a good stability for these molecules.

3.1.2. Red, orange, pink and purple

The madder samples (*R. akane*, *R. cordifolia* and *R. tinctorum*) showed the typical distribution of anthraquinones. Alizarin, xanthopurpurin, rubiadin, purpurin, anthragallol, munjistin and pseudopurpurin were present in the three samples and munjistin showed the highest relative abundance in all of them. However, munjistin was extremely predominant in *R. cordifolia* and alizarin showed remarkably higher relative abundance in *R. tinctorum* than in the other species. Additionally, 6-hydroxyrubiadin was only detected in *R. akane* and nordamnacanthal was only detected in *R. tinctorum*. Glycosides also showed differences amongst the species: 6-hydroxyrubiadin primveroside ($[M-H]^-$ = 563.141 *m/z*), 6-hydroxyrubiadin rhamnosyl glucoside ($[M-H]^-$ = 577.156 *m/z*) and its acetate derivative ($[M-H]^-$ = 619.167 *m/z*) were specific for *R. akane*, whereas ruberythric acid ($[M-H]^-$ = 533.130 *m/z*), rubiadin primveroside ($[M-H]^-$ = 547.146 *m/z*) and lucidin primveroside ($[M-H]^-$ = 563.141 *m/z*) were characteristic of *R. tinctorum*. Negligible amounts of glycosides were observed for *R. cordifolia*. These results were in good agreement with the ones presented by Mouri and Laursen [61] and the chromatographic profiles are shown in Fig. 5. After artificial ageing, the relative abundances of some of the molecules changed slightly, but generally a good consistency was shown, with all the markers still present. The set of reference samples also included an iron-mordanted sample dyed with *R. tinctorum*. It was interesting to observe that no significant difference in the molecular composition was present between the alum-mordanted and the iron-mordanted samples, despite a very different colour.

In contrast, the two samples obtained from sappanwood (*B. sappan*) dyed at neutral and alkaline pH showed some differences in composition. The chromatographic peaks for brasilin and brasilein, known as markers for this dye [8,27,62], showed high relative abundances in the sample dyed at neutral pH (bright red). Other molecules, such as sappanol, 3-deoxysappanchalcone, sappanone A and B, 3-deoxysappanone B and some of their isomers also showed significant abundances [63], as well as protosappanins, especially D and E. On the other hand, the so-called type C component had a very low abundance in this sample. This compound has recently been identified as a benzochromenone referred to as urolithin C [64]. The sappanwood sample dyed at alkaline pH (bright fuchsia) showed a much higher relative abundance of urolithin C than the sample dyed at neutral pH with comparison to brasilin and brasilein. In addition, a much lower abundance of protosappanins was found in this sample. After artificial ageing, a drastic reduction of brasilin and brasilein was observed with a corresponding relative increase in the relative abundance of urolithin C. However, the formation of this compound does not appear to be directly related to the

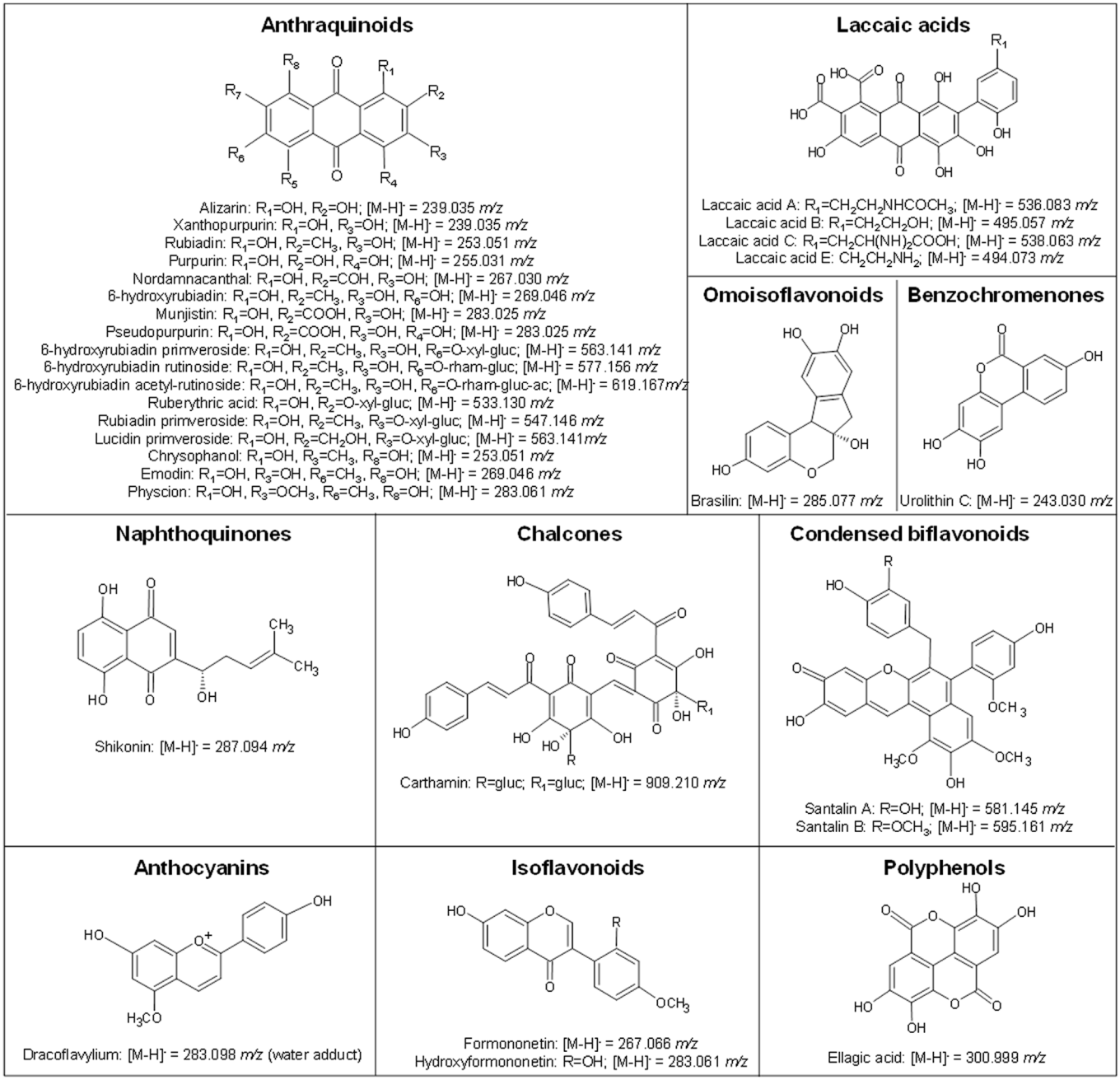

Fig. 3. Molecular structures, names and *m/z* values of the molecular ions of most molecules discussed as responsible for orange/red/pink/purple/brown colours. The molecules are divided into categories. Table S1 reports additional mass spectrometric details and the botanical sources of the molecules.

degradation of brasilin and brasilein [64]. Therefore, urolithin C might naturally be present in the sappanwood heartwood and its extraction is likely to be affected by pH conditions. Further studies are needed to clarify this aspect better, but the stability of urolithin C appears to be intrinsic to its molecular structure and it can therefore be considered as the most reliable marker for the identification of sappanwood in aged samples. However, other types of red dyewoods, including brazilwood (*Caesalpinia echinata*) and other *Caesalpinia* spp., produce a dye with an extremely similar composition to sappanwood (*B. sappan*) and urolithin C is the markers of identification of these plants as well. As these other plants are originally from South America, a correct identification can therefore only be achieved if the geographical origin and date of the textiles are certain. The chromatographic profiles of the sappanwood reference samples are shown in Fig. 11a–c, where they are compared with some profiles obtained for the archaeological samples (see section 3.2.2).

The samples obtained from sandalwood (*P. santalinus*) in neutral and alkaline dyeing conditions did not show significant differences in composition. The results presented here were similar to the ones obtained by Surowiec et al. [65]. Santalins, in particular A, B, C and AY were detected, with santalins A and B being the most abundant. Pterostilbene was also present in significant abundance, together with some chalcones and isoflavones, namely formononetin, butin, butein, angolensin, anisoin, hydroxyformononetin and some unidentified ones. The lack of detection of santarubins confirmed the attribution to *P. santalinus*, which does not contain these molecules unlike other red insoluble dyes (*Baphida nitida*) [65,66]. Santalins were not detected after artificial ageing. This makes this dye difficult to identify, particularly because formononetin, butin and butein are common to other plants that can be used to obtain red/brown colours, such as rosewood (*Dalbergia*

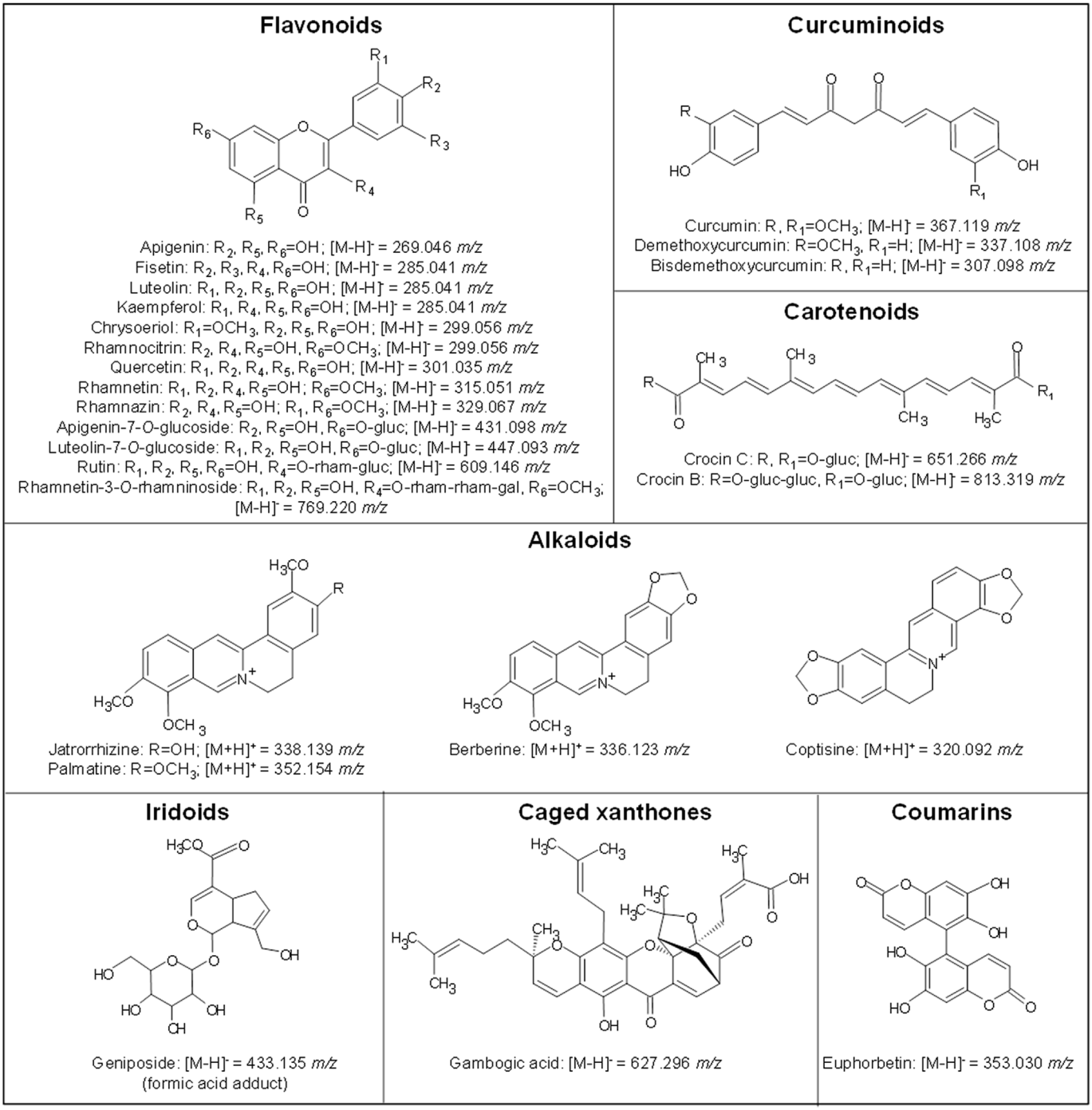

Fig. 4. Molecular structures, names and *m/z* values of the molecular ions of most molecules discussed as responsible for yellow colours. The molecules are divided into categories. Table S1 reports additional mass spectrometric details and the botanical sources of the molecules.

sp.) [67]. Electrospray ionisation mass spectrometry has been applied for the characterisation of flavonoids and neoflavonoids in *Dalbergia odorifera* extracts [68]. The results present here were in agreement with this previous research and liquiritigenin, isoliquiritigenin, pinocembrin, formononetin, butin, butein, melanettin, hydroxyformononetin, prunetin, vestitione, koparin, sativanone, stevenin, violanone and 3′-*O*-methylviolanone were identified as the main components of the dye produced from the raw material. Various unidentified (poly)hydroxy (poly)methoxyisoflavones were also present. After artificial ageing the relative abundance of the molecules decreased significantly, reflecting the high level of fading of this dye, but the internal proportions remained similar. Hydroxybenzoic acids also appeared as degradation products of the flavonoids. Fig. 6 shows the chromatographic profiles of the non-aged sandalwood and rosewood samples.

Lac dye (*K. lacca*) showed the typical composition frequently described in the literature, with laccaic acids A, B, C, D and E showing high abundances [25]. Xantholaccaic acids A ($[M\text{-}H]^-$ = 520.0885 *m/z*) and B ($[M\text{-}H]^-$ = 479.0620 *m/z*) were also present [69], as well as an unidentified compound with $[M\text{-}H]^-$ = 634.0686 *m/z*. The tandem mass spectrum suggested that the structure of this compound is related to the other laccaic acids, as they share the main fragment ions, namely $[M\text{-}H_2O]^-$, $[M-H_2O-CO_2]^-$, $[M-H_2O-CO_2-CO_2]^-$ and $[M-H_2O-CO_2-CO_2-H_2O]^-$. The unidentified laccaic acid also shows a fragment ion corresponding to $[M-H_2O-CO_2-CO]^-$, which points

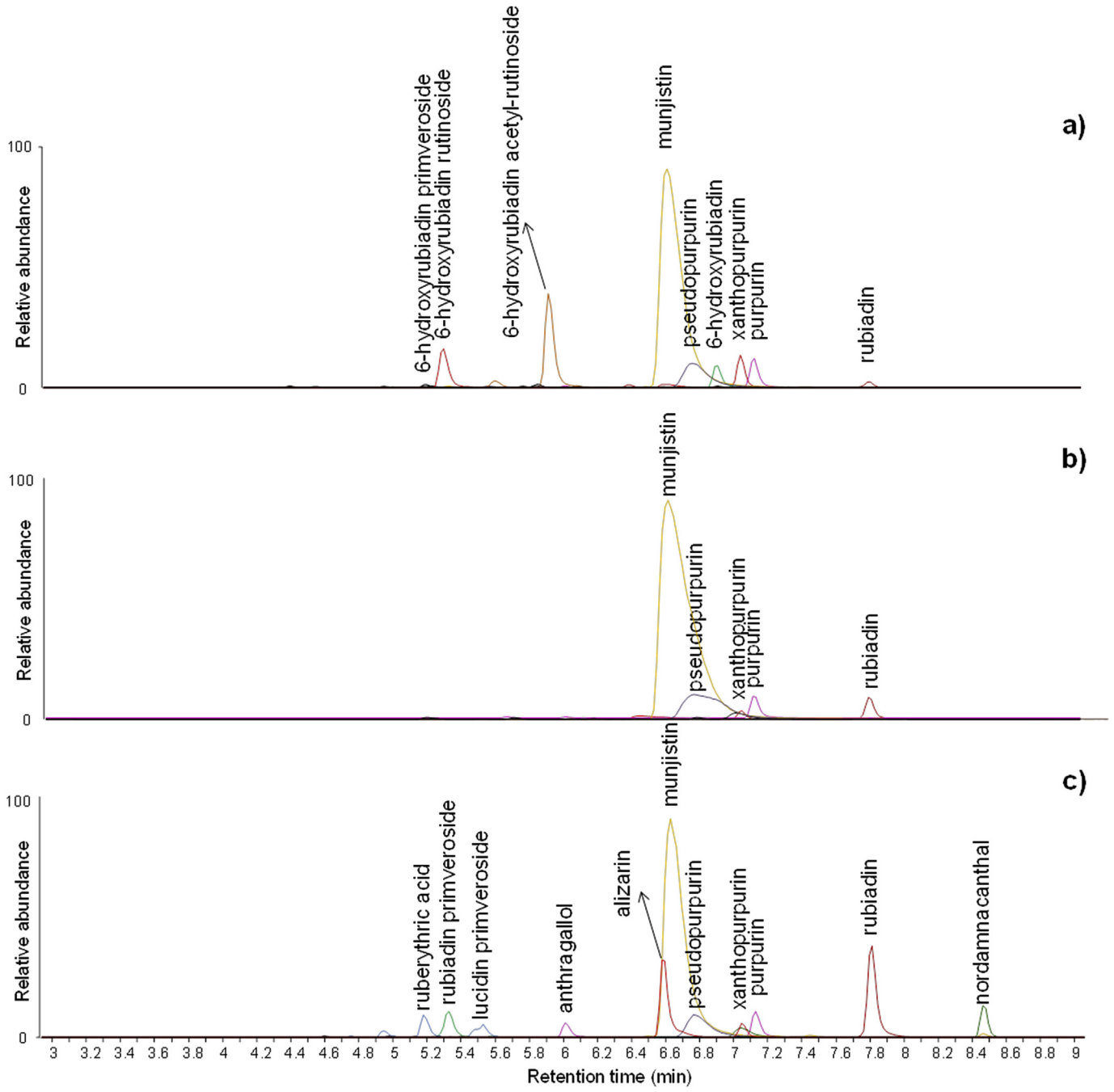

Fig. 5. Extract ion chromatograms of the anthraquinones detected by HPLC-ESI-Q-ToF analysis (negative mode) of **a)** Japanese madder (*R. akane*), **b)** Indian madder (*R. cordifolia*) and **c)** dyer's madder (*R. tinctorum*).

towards the presence of an additional CO group on the molecule, but the interpretation could not provide further information. As recently described, lac dye is usually present with associated compounds from shellac resin [25,70,71], such as polyhydroxy carboxylic acids (aleuritic acid, butolic acid, etc.), sesquiterpenoid acids (jalaric acid, laccijalaric acid, shellolic acid, etc) and their esters and polyesters. This sample was no exception. Although lacciaic acids A and B are reported to be prone to the degradation, the distribution of the compounds after artificial ageing was very similar to the non-aged sample. Dragon's blood (*Daemonorops* sp.) is another material that shares the co-presence of resinous compounds and colourant molecules [72]. Many triterpenes were detected in the reference sample, in agreement with what is reported in the literature [73]. The main colourant molecules were trihydroxychalcone, dihydroxymethoxychalcone, dracoflavylium, 4,6-dihydroxy-2-methoxy-3-methyldihydrochalcone, dracooxepine, dracoflavan A, B1 and B2 [72,74]. The identification of dracoflavylium and other anthocyanins by electrospray ionisation in negative mode is generally complicated, as these molecules tend to form water adducts and dracoflavylium was in fact detected in this form [75]. The formation of formic acid adducts in the ESI source is also a possibility for other classes of molecules, as addressed in section 3.1.3. Dracoflavylium is considered the marker for *Daemonorops* plants, which can be distinguished from *Dracaena* and other plants producing dragon's blood [76]. After artificial ageing, the composition was significantly different. Dracoflavans were absent and additional peaks were present. These were not identified, but are likely to be degradation products of flavonoids and triterpenes.

Gromwell (*L. erythrorhyzon*) is the most common source of purple in

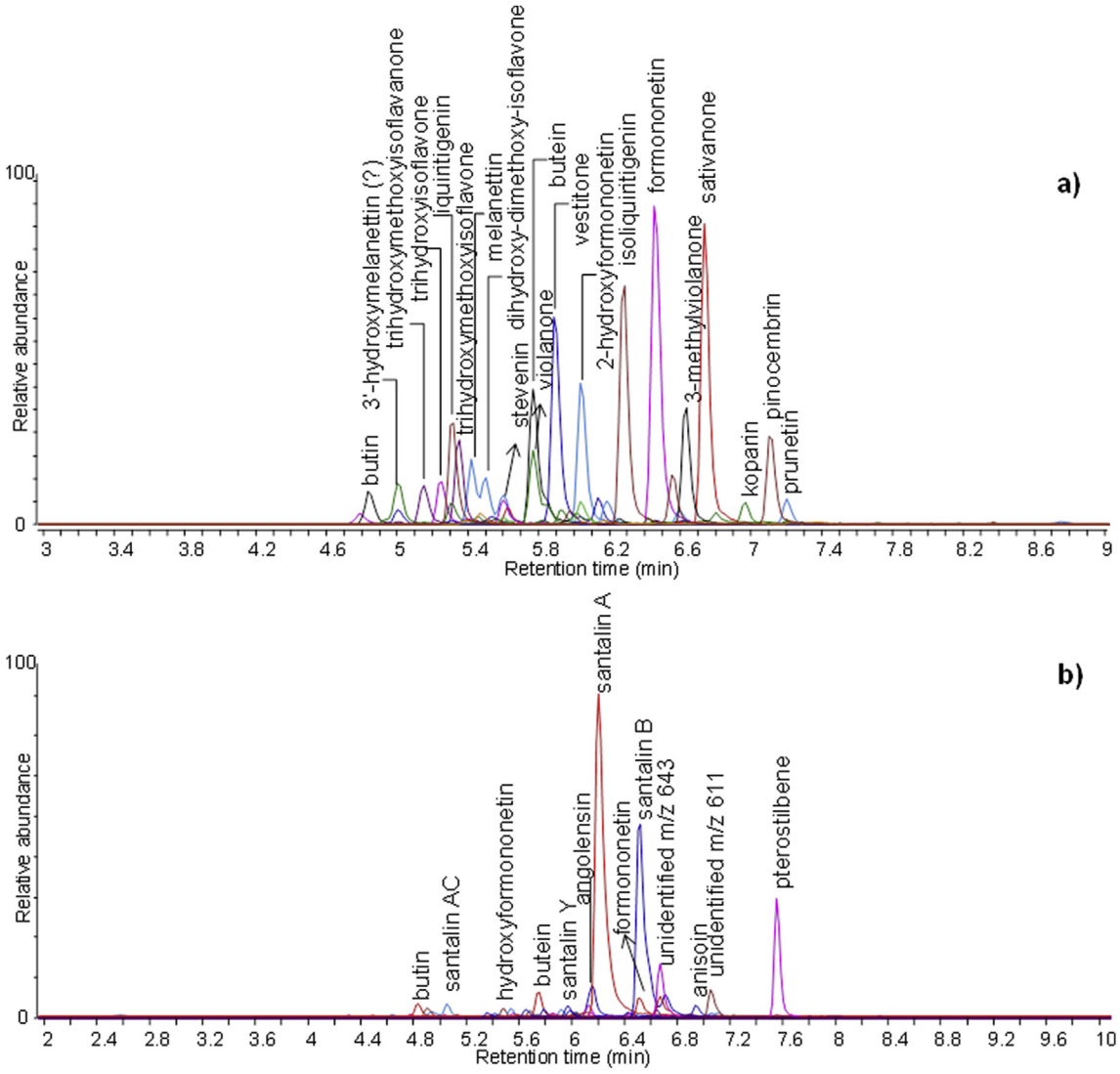

Fig. 6. Extract ion chromatograms of the molecule detected by HPLC-ESI-Q-ToF analysis (negative mode) of **a)** rosewood (*Dalbergia* sp.) and **b)** sandalwood (*P. santalinus*).

Asia [1]. Gromwell's molecular marker is shikonin. Many other molecules are reported in the fresh extract of gromwell and other *Boraginaceae* plants [77,78], but these do not appear to be present in the extracts obtained from dyed textiles, probably suggesting a poor affinity of these molecules for the fibres or the difficulty to extract them from the plant. Shikonin is considered the marker for the identification of gromwell, but this naphthoquinone is an optical isomer of alkannin, which is the molecular marker for alkanet (*Alkanna tinctoria*) and is found in other purple-dyeing plants, such as *Onosma* and *Arnebia* spp. As alkannin and shikonin cannot be separated on reverse phase HPCL or distinguished by ESI-MS, the differentiation of all these species is not straightforward and the geographical origin of the textile plays a role in the identification. Nevertheless, three other molecules were found together with shikonin in the reference sample of gromwell, their $[M\text{-}H]^-$ being 205.014 *m/z* ($C_{10}H_6O_5$), 259.025 *m/z* ($C_{13}H_8O_6$) and 285.077 *m/z* ($C_{16}H_{14}O_5$). Shikonin was found with very low abundance after ageing, whereas the other three compounds still showed significantly high abundances, which makes them reliable markers for gromwell in aged samples, assuming they are not present in the other above-mentioned purple-dyeing plants. The tandem mass spectra did not give sufficient information to elucidate the structures completely. However, the fragmentation of the $C_{10}H_6O_5$ molecule points towards a trihydroxynaphthoquinone and the fragmentation of the $C_{13}H_8O_6$ molecule suggests a tetrahydroxyxanthone or tetrahydroxybenzochromenone as possible structures.

The main red component of the safflower dye (*C. tinctorius*) is carthamin, which is always found with two degradation products. These are the result of a reverse aldol condensation [79,80]. The masses of their $[M\text{-}H]^-$ are 449.109 ($C_{21}H_{22}O_{11}$) and 477.104 ($C_{22}H_{22}O_{12}$) *m/z*. Another non-coloured component with $[M\text{-}H]^- = 582.262$ ($C_{21}H_{45}NO_{17}$) *m/z* was present in all the safflower samples, including the yellow reference [79,81]. In the yellow sample apigenin and kaempferol were also detected, as well as some quinochalcones, including safflower yellow A and hydroxysafflower yellow A. The composition of the yellow safflower sample did not change significantly after ageing, whereas for the red safflower, which is known to be highly fugitive, carthamin was very low compared to the two degradation products and the compound with $[M\text{-}H]^- = 582.262$ *m/z*. Therefore, these compounds are more reliable markers than carthamin in very faded samples. The chromatographic profiles of the pink safflower reference sample before and after ageing are shown in Fig. 9e–f, where they are compared with some profiles obtained for the archaeological samples (see section 3.2.2).

3.1.3. Yellow

Rhubarb (*R. emodi*) extracts contain anthraquinones and

anthraquinone glycosides, but also stilbenes, sennosides and galloyl-glycosides [82,83], which contribute to produce brownish yellow/orange colour. The stilbenes resveratrol, deoxyrhapontigenin, piceatannol and rhapontigenin were all found in their aglycone, glycoside and galloyl-glycoside forms and the same was obtained for the anthraquinones chrysophanol, emodin and physcion. *P*-coumaryl glycosides and trigalloyl-glucose were also identified. The high relative abundance of stilbenes and the absence of rhein confirmed the attribution to *R. emodi* [83]. All the compounds were detected after ageing, although a relative decrease in the glycosides and differences in the relative abundances of most molecules were observed.

Turmeric (*C. longa*) composition has been widely studied and the curcuminoid compounds characterised [84,85]. Curcumin, demethoxycurcumin and bisdemethoxycurcumin can be considered the three markers for this dye, but the non-aged sample contained other triplets of curcuminoids ($[M\text{-}H]^-$ = 321, 351 and 381 *m/z*, and $[M\text{-}H]^-$ = 445, 475 and 505 *m/z*) with much lower relative abundances [85]. These compounds were not identified with certainty. Turmeric was the most light-sensitive dye in this investigation and after ageing the colour was almost completely gone. However, traces of curcumin, demethoxycurcumin and bisdemethoxycurcumin were still detected after ageing.

Saffron (*C. sativus*) and cape jasmine (*G. jasminoides*) both contain carotenoids, among which crocin-related molecules are responsible for the colour. Crocin A, B, C, E and F share the same crocetin skeleton but have different number of glucose substituents [86]. In these analyses crocin B (three glucose substituents) and crocin C (two glucose substituents) were identified in both saffron and cape jasmine samples, as well as their formic acid adducts, the masses of their $[M\text{-}H]^-$ being 697.271 ($C_{33}H_{46}O_{16}$) and 859.324 ($C_{39}H_{56}O_{21}$) *m/z*. Two other unidentified compounds ($[M\text{-}H]^-$ = 510.187 and 533.188 *m/z*) were detected with high relative abundance in both saffron and cape jasmine samples. Although the structure was not elucidated, the tandem mass spectra revealed that these molecules are also crocetin derivatives, as the fragment ion corresponding to the crocetin molecule (*m/z* 327.160 – $C_{20}H_{24}O_4$) was present in both MS/MS spectra. Crocin A, pirocrocin and crocetin, which are reported in other works [27,86], were not identified. Saffron showed the presence of kaempferol glycosides and kaempferol-3-sophoroside [87], which were not detected in the cape jasmine sample. On the other hand, cape jasmine showed the presence of some iridoid molecules, such as geniposide (formic acid adduct with *m/z* 433.135), 6′-*trans*-sinapoyl geniposide, 6″-*O*-*p*-coumaroyl-genipin-gentiobioside and 6′-*O*-*trans*-sinapoyl-genipin gentiobioside and some phenolic acids, such as dicaffeoylquinic acid, 5-*O*-caffeoyl-4-O-sinapoylquinic acid and 3,5-di-*O*-caffeoyl-4-*O*-(3-hydroxy-3-methyl)-glutaroylquinic acid [88]. These were not present in the saffron sample. Geniposide, which was the most abundant peak in the chromatogram of the cape jasmine sample before ageing, showed a drastic reduction after ageing. All the other molecules were detected for both the saffron and cape jasmine samples after ageing. The chromatographic profiles of saffron and cape jasmine are shown in Fig. 7.

The coloured molecules of gamboge (*G. hanburyi*) are referred to as caged xanthones. Forbesione, morelloflavone, morellic and isomorellic acid, gambogenin and isogambogenin, hydroxygambogic acid, neogambogic acid, hydroxyneogambogic acid, spicataside and morelloflavone glucoside were detected in this sample [89,90]. *S* and *R* isomers were generally present as separate peaks. A similar composition was obtained for the aged sample.

Amur-cork tree (*P. amurense*), Japanese barberry (*B. thunbergii*) and Chinese goldthread (*C. chinensis*) belong to the same class of dyes, namely protoberberine dyes. They contain alkaloids, which do not ionise in negative mode, as they are positively charged due to the presence of a quaternary nitrogen atom. Therefore, these three samples were only investigated in positive mode. They all contained berberine, palmatine and jatrorrhizine among the most abundant components, but Chinese goldthread was the only one containing coptisine, which can be used as a marker for identification [91,92]. Japanese barberry has a higher content of jatrorrhizine [91,93] and two unidentified compounds were detected in these analyses. The masses of their $[M\text{-}H]^-$ were 298.145 and 305.151 *m/z*. The chromatogram of the amur-cork tree sample was dominated by the berberine peak [91]. Many other minor protoberberines were detected in these samples, including magnoflorine, phellodendrine, magnocuranine, hydroxyberberine, hydroxypalmatine, etc [92,94]. After ageing the amur-cork tree sample showed a significant reduction in berberine and jatrorrhizine, whereas the other samples showed similar compositions. Fig. 8 reports the chromatographic profiles of the three protoberberine dyes before ageing, highlighting the different compositions.

The other dyes under investigation were all flavonoid-based dyes. Smoketree contains sulfuretin, fisetin and fustin, that can be used as markers for its identification [27,95], but butin, butein, quercetin and taxifolin were also detected [95], as well as some gallic acid derivatives. Pagoda tree buds contain quercetin and rutin as main flavonoids, but kaempferol and isorhamnetin are present together with their rutinosides [27,96]. Silvergrass contains apigenin, luteolin and tricin together with some of their *C*-pentosides, *C*-glycosides and di*C*-glycosides [41,97], which makes this dye distinguishable from most of the other yellows. Attention must be paid to the dye obtained from hairy jointgrass (*Anthraxon hispidus*), which has a similar composition and is reported as an alternative grass source of yellow dye [29,41], however, a reference for this dye was not available. Violet also contains apigenin and luteolin *C*-glycosides and di*C*-glycosides [98], but not pentosides, and aesculetin and euphorbetin are present as major components [99]. Symplocos was not used just to obtain yellow shades, but sometimes also as an additive for mordanting/shading colours, as it is naturally rich in aluminium. The composition obtained in these analyses was very complex, with afzelechin, catechin, quercetin and isoquercitrin identified as the main flavonoids [100]. A series of not fully elucidated molecules were detected and these were likely to be ascribed to the saponines reported to be present in this plant [101].

Buckthorn and weld were also included in the set of reference dyes. These sources of dyes are known to be quite common in the European tradition [1]. Nevertheless, *Rhamnus* plants grow in China and are mentioned as possible sources of yellow dyes [29,102]. The composition of the flavonoids extracted from the berries is slightly variable depending on the species of the plant, but characteristic molecular markers are present in most species. These are rhamnocitrin, rhamnetin, isorhamnetin, rhamnazin and all their rhamninosides (rhamnosyl-rhamnosyl-galactosides) [103,104]. After ageing, the relative abundance of the aglycones compared to glycosides increased, but all molecules were detected. Weld is not a typical Chinese plant but there are publications describing the detection of luteolin-based yellow dyes in Chinese textiles with a very similar composition to weld [22,35,38]. In fact, luteolin, apigenin, chrysoeriol, their *O*-glycosides and di-*O*-glycosides are the main components of weld [105] and this was in agreement with the results obtained. Diglycosides are drastically reduced during ageing but the identification usually relies on both aglycones and glycosides.

There are at least two other important sources of yellow dyes from Asia. The so-called desert poplar (*Populus euphratica* or *Populus pruinosa*) contains apigenin, luteolin and chrysoeriol similarly to weld, but the glucuronides of these molecules are also reported as signature markers for this dye source [35]. Larkspur (*Delphinium semibarbatum*) contains kaempferol, quercetin and isorhamnetin glycosides as molecular markers [2,42]. These two plants were not available in the set of reference samples, but they are included in Table S1 (Supplementary Information) using data from the literature for completeness of information [35,42].

3.2. Archaeological samples

The results obtained from the HPLC-MS analysis of the samples taken from the archaeological textiles are summarised in Table 1, which

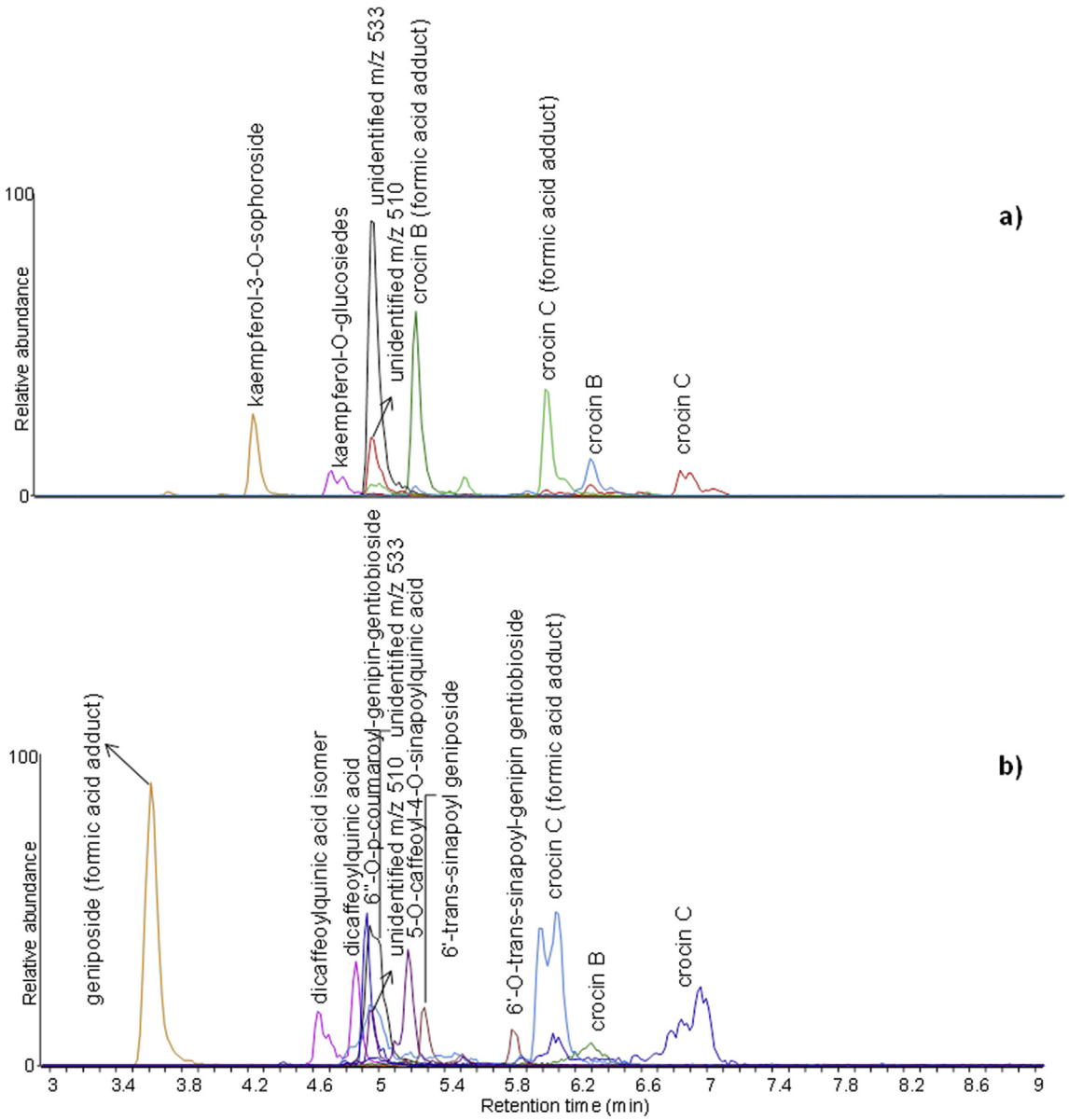

Fig. 7. Extract ion chromatograms of the molecule detected by HPLC-ESI-Q-ToF analysis (negative mode) of **a)** saffron (*C. sativus*.) and **b)** cape jasmine (*G. jasminoides*).

also shows the level of information already achieved using FORS and multispectral imaging [16]. Based on these non-invasive results, the coloured areas to be sampled were selected, including unidentified colours and dye sources to be confirmed more precisely.

3.2.1. Monochrome textiles

MAS.939 and MAS.954 were both bright red (Fig. S1, Supplementary Information). The presence of a plant-based red was suggested by FORS for MAS.954, but inconclusive results were obtained non-invasively for MAS.939 (Table 1). Sample analysis revealed the presence of dyer's madder (*R. tinctorum*) in sample MAS.939 and a mixture of Indian madder (*R. cordifolia*) and sappanwood for MAS.954. The identification of dyer's madder was based on the detection of ruberythric acid, lucidin primveroside and alizarin with high relative abundances compared to the other anthraquinones, whereas Indian madder was identified based on high relative abundances of rubiadin and munjistin and the absence of alizarin [35,61]. Nevertheless, attention must always be paid when trying to distinguish between different madders in archaeological samples, as ageing, dyeing recipes and overdyeing can affect the final composition of the dye. Surprisingly, dyer's madder was also detected in all the purple samples (MAS.891, 900, 901, 902, 903 and 937) together with gromwell, which was already suggested from non-invasive analyses (Table 1). Another example of gromwell mixed with a red dye (sappanwood) was found in the purple colour of the Dunhuang embroidery “Sakyamuni preaching on Vulture Peak” [22]. These mixtures might be deliberate to obtain a certain shade of purple, but they could also highlight the fact either that gromwell was an expensive dye or that dyeing with gromwell was not easy, due to the poor water solubility of the colourant molecules. Therefore, adding reds might have reduced the price and mitigated the difficulty of the dyeing practice, and might be a signature for textiles produced in Dunhuang.

Gromwell was also detected in MAS.869 and MAS.949, which had brown colourations. In MAS.869 it was found mixed with both madder and sappanwood and in MAS.949 it was found mixed with lac dye. The identification of the lac dye in this case was not based on the detection of laccaic acid A, but on the presence of many shellac markers. These, as previously shown, can be used as markers of identification of lac dye by

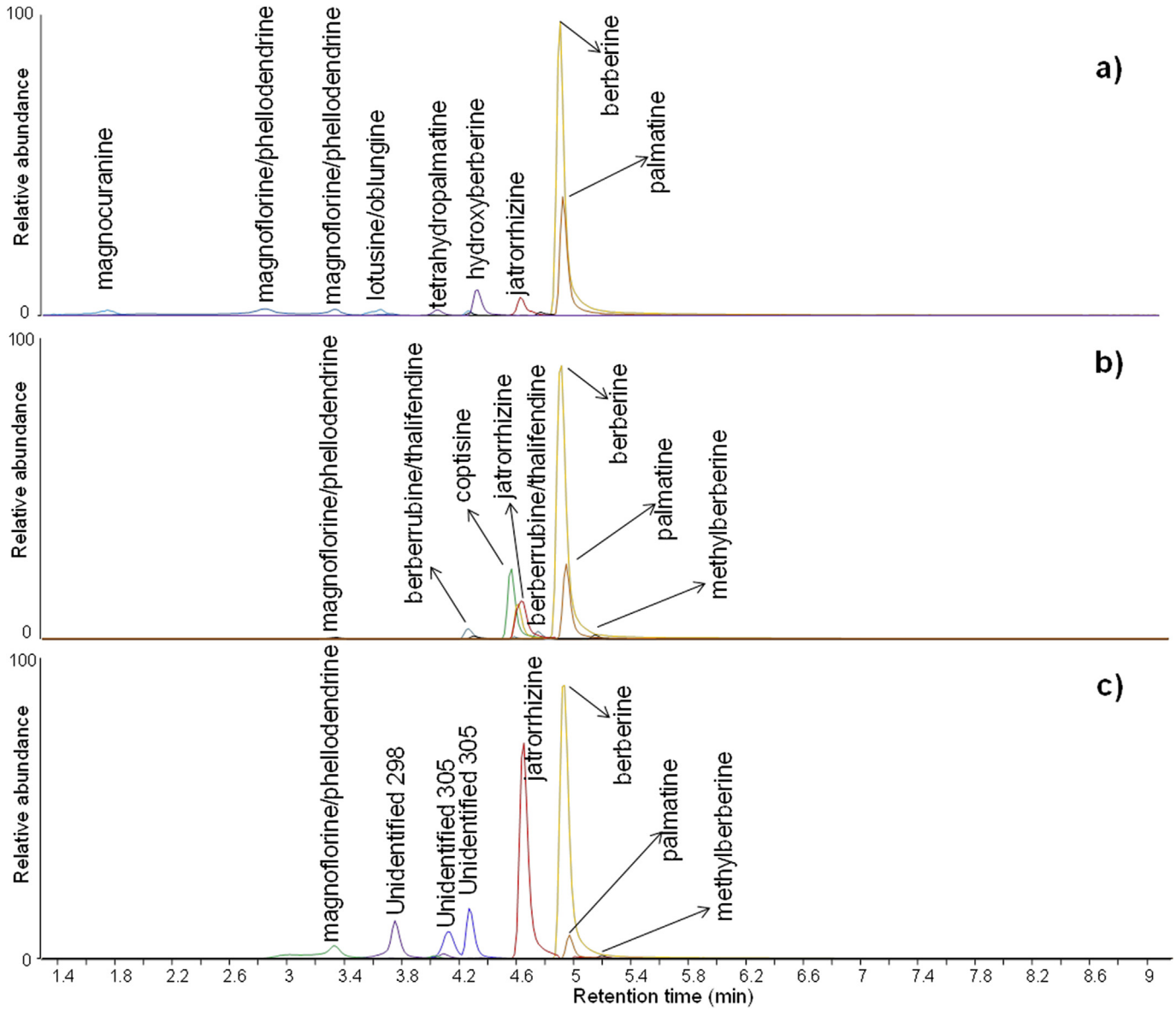

Fig. 8. Extract ion chromatograms of the alkaloids detected by HPLC-ESI-Q-ToF analysis (positive mode) of **a)** amur-cork tree (*P. amurense*), **b)** Chinese goldthread (*C. chinensis*) and **c)** Japanese barberry (*B. thunbergii*).

HPLC-MS [70], when the laccaic acids have degraded. The brownish colours are consistent with an advanced degradation of gromwell, which is known to turn brown after long exposure to light [16].

MAS.904 and MAS.951 exhibited an orange colour, which was identified as safflower, as already suggested by the bright orange luminescence observed in UV-induced luminescence images [16]. Carthamin, its degradation products and the unidentified compound with *m/z* 582 were all identified, but differences were observed in their relative abundances. Safflower was also identified in some of the yellow textiles (MAS.936 and MAS.938). No safflower yellow components were detected, thus indicating an original orange/pink colour of these textiles, which has faded over time. Considering the differences in the relative abundance of the four compounds detected, an interesting trend was noticed, which appeared to be related to the fading of the safflower dye. In fact, the relative abundance of carthamin compared to its degradation products progressively decreases with the fading, as clearly visible in Fig. 9 and in agreement with other studies [79,80]. With an appropriate dataset, these ratios can potentially be used to establish the extent of the fading of this dye.

For the other yellow textiles (MAS.890, MAS.935 and MAS.942), MAS.935 was the only one with a secure identification from the non-invasive analysis, as the bright yellow luminescence in UV-induced luminescence images had already suggested the presence of a proto-berberine-based dye (Table 1). This was confirmed by the detection of berberine, jatrorrhizine and hydroxyberberine, with berberine showing the highest relative abundance. The almost complete absence of palmatine can be taken as an indication of the possible use of *Phellodendron chinense* (Chinese cork tree) rather than *Phellodendron amurense* (amur-cork tree) [91], as also observed in other studies [35]. MAS.942 was dyed with pagoda tree buds, as suggested by the detection of rutin, and MAS.890 was dyed with a mixture of smoketree and pagoda tree buds, as fustin, sulfuretin, butin and butein were also found together with rutin.

The presence of mixtures of dyes is very consistent in the results obtained from the monochrome textiles. These mixtures cannot be easily picked up by FORS and multispectral imaging, especially in the case of over-dyeing, as these techniques respond to the surface composition of the fibres. Therefore, the extraction of dyes from samples is required in order to obtain this detailed information. Over-dyeing was also suggested by microscopical observations of the samples, where only one

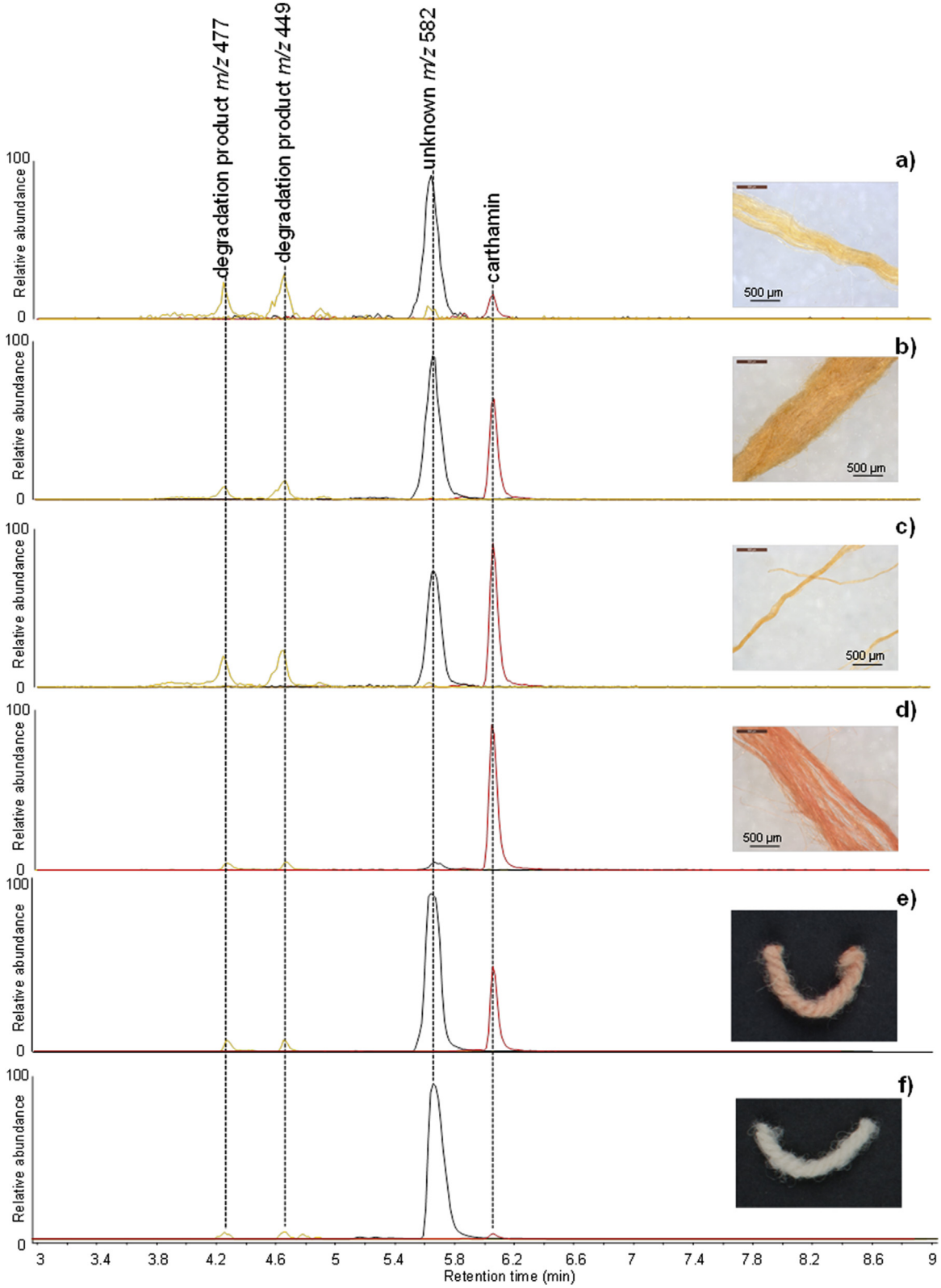

Fig. 9. Extract ion chromatograms of red safflower components obtained by HPLC-ESI-Q-ToF analysis (negative mode) of **a)** MAS.936, **b)** MAS.938, **c)** MAS.904, **d)** MAS.951, **e)** non-aged reference sample and **f)** aged reference sample, showing the correlation of the relative abundance of carthamin to the fading.

colour was generally observed. Considering the use of these textiles as fragments to produce banners and canopies as forms of patchwork [44], it is reasonable to believe that they had been recycled and possibly re-dyed during their lifetime to refresh the colour or change the hue. Therefore, the mixtures detected are probably representative of different phases/uses of these textiles, especially when two similar colours (two reds or two yellows) are found on them.

3.2.2. Polychrome textiles

For MAS.865 (Fig. S2, Supplementary Information) one orange

sample was taken from the front of the textile together with a corresponding red sample taken from the back. Both samples showed urolithin C, brasilin, brasilein, sappanol and protosappanin B, D and E, highlighting sappanwood as source of the red dye (Fig. 11d). This was in disagreement with the results obtained non-invasively, as safflower was suspected in this sample (although not clearly identified), because of the orange luminescence observed. However, no trace of safflower molecules was found. A yellow sample was also taken and this was the only example of an unidentified yellow in these textiles. Luteolin-7-*O*-glucoside and isoquercitrin (quercetin-3-*O*-glucoside) were identified and two other unidentified molecules were detected, showing $[M-H]^-$ with *m/z* 433.114 ($C_{21}H_{22}O_{10}$) and *m/z* 449.109 ($C_{21}H_{22}O_{11}$). The MS/MS spectra enabled the partial identification of these compounds, as the main fragment ions at 271.061 and 287.056 *m/z* respectively indicated the loss of a glucose molecule (162 u). These were therefore *O*-glucosides of two molecules with formula $C_{15}H_{12}O_5$ and $C_{15}H_{12}O_6$ respectively, probably trihydroxy- and tetrahydroxyflavones, but no further interpretation can be achieved. Naringenin could be an option for the former molecule [106], and this is mentioned as a possible marker for the use of tangerine yellow from *Citrus reticulata* or *Citrus tangerina* [34], but this was not confirmed by using a standard. Traces of some of these molecules were found in the orange sample from MAS.865 and the same unidentified source of yellow dye was found in the yellow and orange (mixed with sappanwood) samples from MAS.873. Also in the case of the orange sample from MAS.873, safflower was actually expected from the non-invasive analysis (Table 1), suggesting that a mixture of sappanwood and this unidentified source of yellow could produce a weak orange luminescence, which can be mistaken for safflower. This will require further investigation and further highlights the importance to use complementary techniques in such investigations. Fig. 10 shows the chromatographic profile of the yellow sample from MAS.865 and the MS/MS spectra of the two unidentified molecules.

Safflower had already been identified non-invasively in MAS.869 (Fig. S3, Supplementary Information), therefore yellow, green and purple samples were taken. The dye from the pagoda tree buds was identified in both the yellow and the green samples (mixed with indigo), by detecting rutin and isorhamnetin rutinoside. Gromwell was identified in the purple sample, as shikonin, emodin and the three not fully identified markers with *m/z* 205, 259 and 285 were detected. This was the only example of pure gromwell in the entire set of purple samples. Similar results were obtained for MAS.871 (Fig. 2a): safflower was identified for the red and pink colours (high relative abundance of carthamin indicated very good preservation), pagoda tree buds for the yellow and green (mixed with indigo) colours, and gromwell was found to be mixed with sappanwood to obtain the purple. MAS.872 (Fig. 2b) was sampled for red (front and back), yellow and green. Sappanwood was identified in the red (Fig. 11e) and larkspur in the yellow and green (mixed with indigo), by detecting kaempferol-3-*O*-glucoside, quercetin-3-*O*-glucoside and isorhamnetin-3-*O*-glucoside. As already mentioned, the yellow from MAS.873 (Fig. S4, Supplementary Information) was not identified (same as MAS.865). This yellow dye was also found mixed with sappanwood in the orange colour, but larkspur was found mixed with indigo to obtain green. This highlighted that yellow and green colours are not always obtained from the same yellow dye, even within the same textile.

MAS.906 (Fig. S5, Supplementary Information) and MAS.908 (Fig. S6, Supplementary Information) were very difficult to sample, because of the way they were woven (kesi technique). The non-invasive approach had already enabled a protoberberine-based dye to be identified in some of the yellow areas of these textiles, as well as safflower, gromwell and tannins [16]. However, a non-luminescent yellow was present in MAS.906, as well as a green colour, which were possible to sample. Pagoda tree dye was identified in the yellow, whereas the identification of the yellow dye used to obtain the green was problematic: luteolin, luteolin-7-*O*-glucoside, apigenin-7-*O*-glucuronide and luteolin-7-*O*-glucuronide were identified, suggesting the presence of the

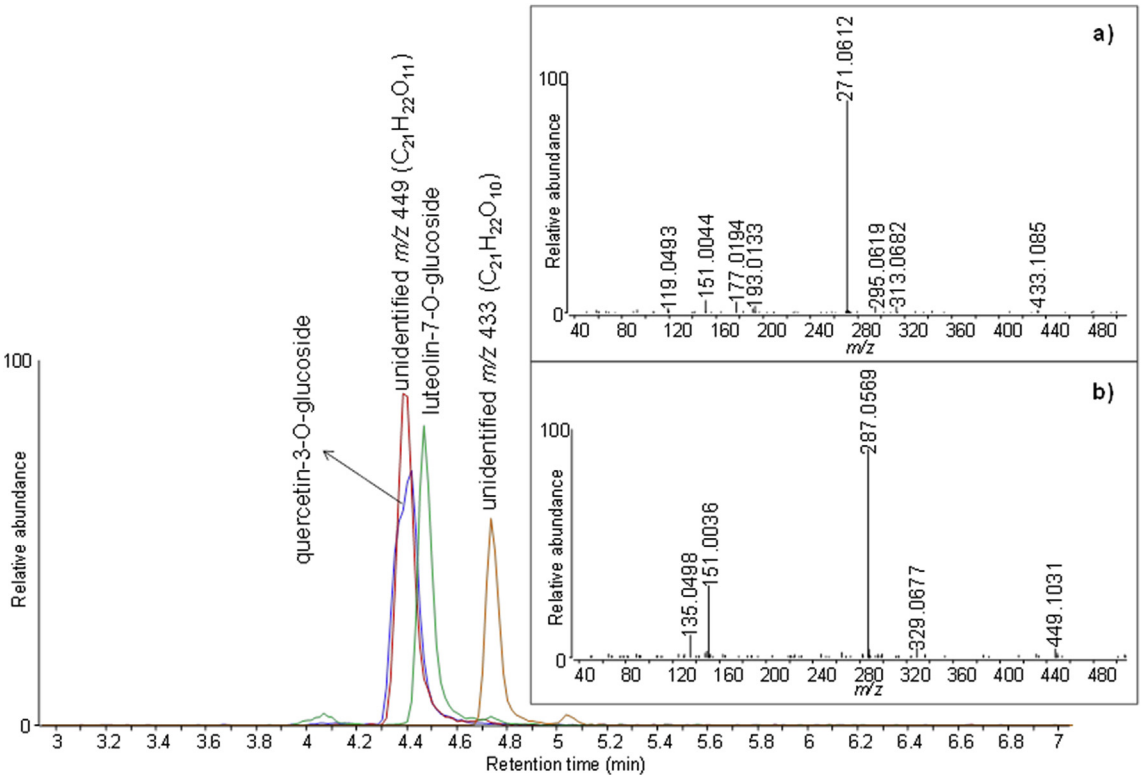

Fig. 10. Extract ion chromatograms of the molecules detected by HPLC-ESI-Q-ToF analysis (negative mode) in the yellow sample from MAS.865. Insets: MS/MS spectra of the two unidentified molecules with **a)** *m/z* 433.114 ($C_{21}H_{22}O_{10}$) and **b)** *m/z* 449.109 ($C_{21}H_{22}O_{11}$). (For interpretation of the references to colour in this figure legend, the reader is referred to the Web version of this article.)

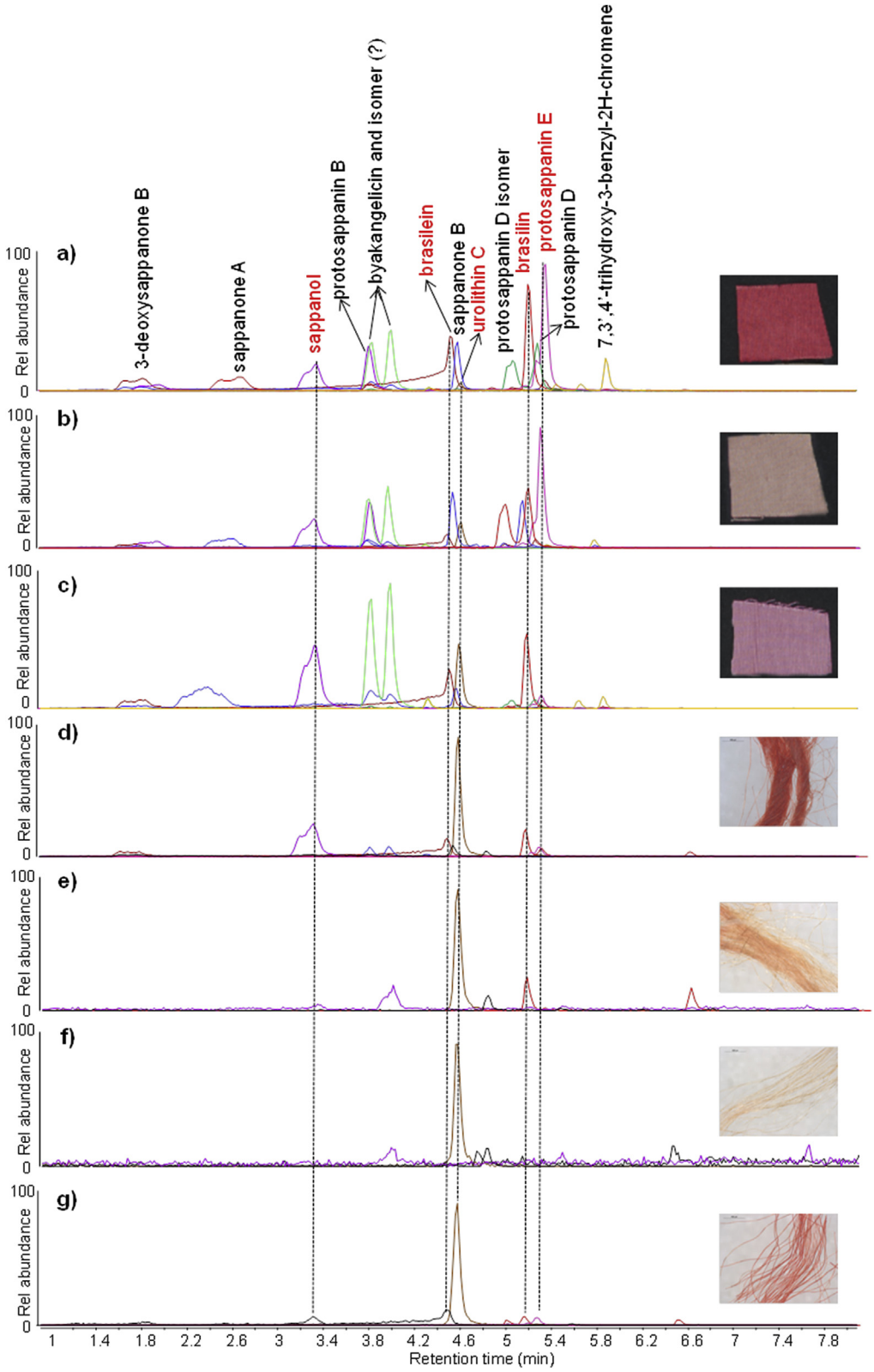

Fig. 11. Extract ion chromatograms of the main sappanwood components obtained by HPLC-ESI-Q-ToF analysis (negative mode) of **a)** reference sample dyed at neutral pH, **b)** aged reference sample dyed at neutral pH, **c)** reference sample dyed at alkaline pH, **d)** MAS.865 (red), **e)** MAS.872 (orange), **f)** MAS.908 (pink) and **g)** MAS.922 (bright red). (For interpretation of the references to colour in this figure legend, the reader is referred to the Web version of this article.)

desert poplar dye. However, the chrysoeriol-7-*O*-glucuronide, which is another main component of this dye, was not detected. An isomer of this molecule with $[M\text{-}H]^-$ = 475.088 *m/z* was detected instead, and its mass spectrum indicated that this was a *C*-glucoside, as suggested by the fragment ions corresponding to $[M\text{-}H\text{-}90]^-$ and $[M\text{-}H\text{-}120]^-$ [41], but no indication about the aglycone molecule was obtained from the spectrum. In addition, orientin (luteolin-8-*C*-glucoside) was also detected. Orientin and luteolin-7-*O*-glucuronide are the main compounds

of the extracts from *Vitex negundo* [107]. As reference samples of desert poplar and *Vitex negundo* were not available, it is difficult to establish which of these sources was used. A mixture of the two is also possible. The same results were obtained for the green sample in MAS.924. The research done to interpret these complex results also enabled the desert poplar dye to be identified in the Dunhuang embroidery "Sakyamuni preaching on Vulture Peak", as apigenin-7-*O*-glucuronide, luteolin-7-*O*-glucuronide and chrysoeriol-7-*O*-glucuronide were identified in a yellow area, but not connected to a specific dye source at the time of the analyses [22].

The pinkish background colour of MAS.908 was also sampled and found to be sappanwood, most likely with a high incidence of fading (Fig. 11f).

For MAS.920 (Fig. S7, Supplementary Information) only the yellow colour was sampled; the pink being already identified as safflower. Weld was identified as possible source of this yellow, as apigenin, luteolin and chrysoeriol were identified, as well as some of their glycosides, but none of the glucuronides, which would have pointed towards the desert poplar dye being present. Moreover, two luteolin-derivative molecules (*m/z* 313.035) were also detected in this sample. These molecules have been recently detected in other works related to Egyptian textiles [15,69] and they are hypothesised to be markers of a different variety of weld or dyeing process used. In fact, weld is not a native plant either of Egypt or China.

For MAS.922 (Fig. S8, Supplementary Information) the bright red of the petals was sampled, as this was not clearly identified by FORS, and sappanwood was identified, by detecting sappanol, brasilin, brasilein, urolithin C, protosappanins D and E (Fig. 11g). In a similar way to what obtained from the samples containing safflower, a certain trend was observed in the samples containing sappanwood, as shown in Fig. 11. The chromatographic profiles of the most saturated reds (MAS.865 and MAS.922) showed several of the sappanwood components, whereas the faded ones tended mainly to show the presence of brasilin and urolithin C. Nevertheless, for all the archaeological samples urolithin C was the most abundant compound, which was not in agreement with the sappanwood reference sample after artificial ageing, for which other compounds were still more abundant. As already mentioned in section 3.1.2, the formation/presence of urolithin C is not fully understood, but fading and exposure to light do not appear to be the only processes involved according to these results.

The yellow from the back of MAS.922 was also sampled and saffron was identified, by detecting kaempferol-*O*-glucoside, the unidentified marker with *m/z* 533, crocin B, crocin C and their formic acid adducts. It was interesting to have an example of the other carotenoid-based dye cape jasmine and confirm the possibility to distinguish it from saffron. In fact, cape jasmine was identified in the yellow area of MAS.929 (Fig. S1, Supplementary Information) and, in addition to the unidentified marker with *m/z* 533, crocin C and its formic acid adduct, some of the iridoids present in the cape jasmine and not present in saffron were detected, such as the formic acid adduct of geniposide, 5-*O*-caffeoyl-4-*O*-sinapoylquinic acid and 3,5-di-*O*-caffeoyl-4-*O*-(3-hydroxy-3-methyl)-glutaroylquinic acid. This proves that these two sources of dyes can be distinguished even in archaeological samples.

MAS.924 (Fig. S9, Supplementary Information) showed yellow, green, greyish/beige and blue stripes. The non-invasive approach was only useful for identifying the indigo. Therefore, samples were taken and yellow was found to be obtained from the pagoda tree buds. However, urolithin C was also identified, probably suggesting the original presence of sappanwood and of a more orange colour faded over time. Urolithin C was also found in the greyish/beige sample together with fisetin, suggesting a mixture of sappanwood and smoketree, which has undergone a high extent of degradation and fading. The green sample contained the desert poplar and/or the *Vitex negundo* dye and indigo. Interestingly, three different sources of yellow were used to obtain three colours in the same textile and they were all mixed with different dyes.

3.2.3. Embroidered textiles

MAS.911 (Fig. S10, Supplementary Information) was virtually impossible to sample without damaging the fine embroidery. Non-invasive analyses already allowed the identification of a protoberberine-based yellow mixed with indigo in the green areas and safflower in the pinkish areas [16]. A sample of the brown ground silk was taken from a loose edge and this turned out to consist of an interesting mixture of madder and a source of condensed tannins, as suggested by the presence of poorly-resolved peaks, showing clusters of *m/z* values around 700–800 *m/z* [108]. In MAS.915 (Fig. S11, Supplementary Information) safflower had been identified in the pink areas and a protoberberine-based yellow mixed with indigo in the green areas [16]. However, the samples of both the light and dark greens that could be taken were the only examples of Japanese barberry (*B. thunbergii*) in these textiles. The identification was based on the relatively high abundance of jatrorrhizine with comparison to berberine and the detection of the unidentified markers with *m/z* 298 and 305, which were also present in the reference sample. A sample of the red was also taken and dyer's madder was identified, as suggested by the presence of high alizarin, nordamnacanthal and ruberythric acid.

Unlike MAS.911, MAS.1130 (Fig. S12, Supplementary Information) provided opportunity for several samples to be taken. Two different sources of yellows were detected: Chinese cork tree and desert poplar, both also mixed with indigo in some green areas. A few pink areas were found to be obtained using lac dye with good preservation state, as indicated by the detection of all laccaic acids. Brownish areas were obtained by mixing madder (probably *R. cordifolia*) with a source of tannins. Madder was also identified in a bright red area and in the purple areas mixed with indigo. This is the only example of obtaining purple with madder and indigo instead of gromwell among these textiles, providing an interesting insight into wide range of dyeing techniques available, some of them probably imported from Mediterranean regions, as mixing madder and indigo is known to be common practice in the production of Roman and Egyptian textiles [15].

4. Conclusions

This work provides a database of mass spectrometric features of molecules to be used for the identification of a wide range of Asian dyes in archaeological textiles. The database was successfully exploited for the dye analysis of more than thirty Chinese textiles from Dunhuang (7th-10th century AD) in the British Museum's collection. This represents an important resource for HPLC-MS users with high applicability not only to Asian colourants but also to dyes from other geographical areas.

The analyses performed before and after ageing were useful in terms of understanding the chemical changes of the most light-sensitive dyes. In fact, the identification of safflower and sappanwood in some archaeological samples was possible only thanks to the detection of degradation products and/or minor components, in agreement with the results obtained on the aged reference samples.

When compared and integrated with the results obtained by a non-invasive approach (microscopy, multispectral imaging and FORS) on the same textiles [16], this paper highlights the delineation of an analytical protocol that can be used on any kind of textiles, if the appropriate reference materials are available. Sampling is fundamental in some cases, in particular for yellow dyes different from protoberberine-based ones, as these cannot be identified non-invasively, but they were successfully characterised here by HPLC-MS. A retrospective look at the multispectral imaging results also highlighted that most of the yellow areas exhibiting an olive-coloured UV-luminescence were dyed with the pagoda-tree bud, suggesting that this olive luminescence can be indicative of the presence of pagoda tree yellow. On the other hand, HPLC-MS results were not in agreement with the non-invasive results in two cases. In fact, a mixture of sappanwood and an unidentified source of yellow appeared to produce an orange UV-luminescence and a FORS

spectrum that can be mistaken for safflower. This further highlights the importance to use complementary techniques whenever possible.

Furthermore, mixtures are sometimes difficult to be discerned non-invasively, especially when they are composed of similarly coloured dyes. Such mixtures were detected in many of the monochrome textiles, highlighting the fact that these textiles had been probably recycled and therefore probably re-dyed during the time they had been used. Gromwell was also found mixed with sappanwood, madder and even with lac dye in most of the purple samples and this pointed towards possible attempts of reducing the cost of the dyeing or overcoming difficulties during the dyeing process.

Most of the dye sources (smoketree, padoga tree, Chinese cork tree, larkspur, saffron, desert poplar, cape jasmine, Japanese barberry, safflower, dyer's madder, Indian madder, sappanwood, gromwell, Indian lac and Chinese sumac) were in accordance with the palette of dyes generally used in the Dunhuang area in this period [29], although some of these dye sources have also been identified in textiles from Ningxia and Xinjiang [34,35,38], showing their use in other parts of China. An example of a weld-like dye pointed towards some possible western sources being used as well. This work also highlights that the dyes were applied in many different ways, which suggests that dyers were experimenting in this period and they adopted techniques not necessarily typical of Asia (for example the mixtures of madder and indigo to obtain purple). These aspects underlined exchange of knowledge and maybe materials (for example weld or a similar plant) along the Silk Road, not only in the direction of Chinese export but also import between the 7th and 10th century AD. Further research expanding the number of textile samples from this and other areas along the Silk Road would help to shed further light on these aspects.

Acknowledgements

The author would like to thank the Getty Conservation Institute (Los Angeles, USA) for providing three of the reference samples. Caroline Cartwright (Scientist, Department of Scientific Research, The British Museum) is thanked for undertaking the SEM examination of the wood anatomy of the *Rhus* sp. sample. Nicole Reifarth (University of Trier, Germany) is thanked for her help in the dyeing process of the reference textiles. Monique Pullan (Head of Organics, Conservation Department, The British Museum) and Yu-Ping Luk (Curator, Asia Department, The British Museum) are thanked for providing access to the archaeological textiles and for their support in the selection and handling of the textiles. As an Andrew W. Mellon Postdoctoral Research Fellow, the author would also like to thank the Andrew W. Mellon Foundation.

Appendix A. Supplementary data

Supplementary data to this article can be found online at https://doi.org/10.1016/j.dyepig.2018.12.025.

References

[1] Cardon D. Natural dyes. Sources, tradition, technology and science. London: Archetype Publications Ltd.; 2007.
[2] Mouri C, Mozaffarian V, Zhang X, Laursen R. Characterization of flavonols in plants used for textile dyeing and the significance of flavonol conjugates. Dyes Pigments 2014;100:135–41.
[3] Ye Y, Salmon LG, Cass GR. The ozone fading of traditional Chinese plant dyes. J Am Inst Conserv 2000;39(2):245–57.
[4] Padfield T, Landi S. The light-fastness of the natural dyes. Stud Conserv 1966;11(4):181–96.
[5] Degano I, Ribechini E, Modugno F, Colombini MP. Analytical methods for the characterization of organic dyes in artworks and in historical textiles. Appl Spectrosc Rev 2009;44(5):363–410.
[6] Pauk V, Barták P, Lemr K. Characterization of natural organic colorants in historical and art objects by high-performance liquid chromatography. J Separ Sci 2014;37(23):3393–410.
[7] Gulmini M, Idone A, Diana E, Gastaldi D, Vaudan D, Aceto M. Identification of dyestuffs in historical textiles: strong and weak points of a non-invasive approach. Dyes Pigments 2013;98(1):136–45.
[8] Manhita A, Ferreira T, Candeias A, Barrocas Dias C. Extracting natural dyes from wool—an evaluation of extraction methods. Anal Bioanal Chem 2011;400(5):1501–14.
[9] Petroviciu I, Albu F, Medvedovici A. LC/MS and LC/MS/MS based protocol for identification of dyes in historic textiles. Microchem J 2010;95(2):247–54.
[10] Rosenberg E. Characterisation of historical organic dyestuffs by liquid chromatography–mass spectrometry. Anal Bioanal Chem 2008;391(1):33–57.
[11] Casadio F, Leona M, Lombardi JR, Van Duyne R. Identification of organic colorants in fibers, paints, and glazes by surface enhanced Raman spectroscopy. Accounts Chem Res 2010;43(6):782–91.
[12] Mounier A, Le Bourdon G, Aupetit C, Lazare S, Biron C, Pérez-Arantegui J, et al. Red and blue colours on 18th–19th century Japanese woodblock prints: in situ analyses by spectrofluorimetry and complementary non-invasive spectroscopic methods. Microchem J 2018;140:129–41.
[13] Nakamura R, Tanaka Y, Ogata A, Masakazu N. Scientific evidence by fluorescence spectrometry for safflower red on ancient Japanese textiles stored in the Shosoin Treasure House repository. Stud Conserv 2014;59(6):367–76.
[14] Nakamura R, Tanaka Y, Ogata A, Naruse M. Dye analysis of shosoin textiles using Excitation−Emission matrix fluorescence and Ultraviolet−Visible reflectance spectroscopic techniques. Anal Chem 2009;81(14):5691–8.
[15] Dyer J, Tamburini D, O'Connell ER, Harrison A. A multispectral imaging approach integrated into the study of Late Antique textiles from Egypt. PLoS One 2018;13(10):e0204699.
[16] Tamburini D, Dyer J. Fibre optic reflectance spectroscopy and multispectral imaging for the non-invasive investigation of Asian colourants in Chinese textiles from Dunhuang (7th-10th century AD). Dyes Pigments 2019;162:494–511.
[17] Pozzi F, Leona M. Surface-enhanced Raman spectroscopy in art and archaeology. J Raman Spectrosc 2016;47(1):67–77.
[18] Derrick M, Newman R, Wright J. Characterization of yellow and red natural organic colorants on Japanese woodblock prints by EEM fluorescence spectroscopy. J Am Inst Conserv 2017;56(3–4):171–93.
[19] Degano I, La Nasa J. Trends in high performance liquid chromatography for cultural heritage. Top Curr Chem 2016;374(2):1–28.
[20] Wouters J, Grzywacz CM, Claro A. A comparative investigation of hydrolysis methods to analyze natural organic dyes by HPLC-PDA - nine methods, twelve biological sources, ten dye classes, dyed yarns, pigments and paints. Stud Conserv 2011;56(3):231–49.
[21] Sanyova J, Reisse J. Development of a mild method for the extraction of anthraquinones from their aluminum complexes in madder lakes prior to HPLC analysis. J Cult Herit 2006;7(4):229–35.
[22] Tamburini D, Cartwright CR, Pullan M, Vickers H. An investigation of the dye palette in Chinese silk embroidery from Dunhuang (Tang dynasty). Archaeol Anthropol Sci 2018. In press.
[23] Lech K, Jarosz M. Identification of Polish cochineal (Porphyrophora polonica L.) in historical textiles by high-performance liquid chromatography coupled with spectrophotometric and tandem mass spectrometric detection. Anal Bioanal Chem 2016;408(12):3349–58.
[24] Gulmini M, Idone A, Davit P, Moi M, Carrillo M, Ricci C, et al. The "Coptic" textiles of the "Museo Egizio" in Torino (Italy): a focus on dyes through a multi-technique approach. Archaeol Anthropol Sci 2016:1–13.
[25] Santos R, Hallett J, Oliveira MC, Sousa MM, Sarraguça J, Simmonds MSJ, et al. HPLC-DAD-MS analysis of colorant and resinous components of lac-dye: a comparison between Kerria and Paratachardina genera. Dyes Pigments 2015;118:129–36.
[26] Petroviciu I, Creţu I, Vanden Berghe I, Wouters J, Medvedovici A, Albu F. Flavonoid dyes detected in historical textiles from Romanian collections. e-Preservation Sci 2014;11:84–90.
[27] Han J, Wanrooij J, van Bommel M, Quye A. Characterisation of chemical components for identifying historical Chinese textile dyes by ultra high performance liquid chromatography – photodiode array – electrospray ionisation mass spectrometer. J Chromatogr A 2017;1479:87–96.
[28] Han J, Quye A. Dyes and dyeing in the Ming and Qing dynasties in China: preliminary evidence based on primary sources of documented recipes. Text Hist 2018:1–27.
[29] Grzywacz CM, Wouters J, Bomin S, Yuquan F. Conservation of ancient sites on the silk Road - Asian organic colourants: a collaborative research project. In: Agnew N, editor. Proc second international conference on the conservation of Grotto sites, Mogao Grottoes. Dunhuang, China: Getty Conservation Institute; 2004.
[30] Zhang X, Laursen R, Osipova S. Analysis of dyes in some 19th-century Uzbek suzanis. In: Kirby J, editor. The diversity of dyes in history and archaeology. London: Archetype Publications; 2017. p. 339–48.
[31] Sasaki Y, Sasaki K. Dye analysis of a 17th-century historic Japanese textile: a non-destructive approach. In: Kirby J, editor. The diversity of dyes in history and archaeology. London: Archetype Publications; 2017. p. 265–77.
[32] Sasaki Y, Koike T, Yano T, Sasaki K. Non-destructive dye analysis for the reconstruction of a 17th-century Haori fragment in the Tokugawa art museum. In: Kirby J, editor. The diversity of dyes in history and archaeology. London: Archetype Publications; 2017. p. 257–64.
[33] Gleba M, Vanden Berghe I, Aldenderfer M. Textile technology in Nepal in the 5th-7th centuries CE: the case of Samdzong. STAR: Sci Technol Archaeol Res 2016;2(1):25–35.
[34] De Luca E, Poldi G, Redaelli M, Zaffino C, Bruni S. Multi-technique investigation of historical Chinese dyestuffs used in Ningxia carpets. Archaeol Anthropol Sci 2016:1–10.
[35] Liu J, Mouri C, Laursen R, Zhao F, Zhou Y, Li W. Characterization of dyes in ancient textiles from Yingpan, Xinjiang. J Archaeol Sci 2013;40(12):4444–9.

[36] Lee J, Kang M, Lee K-B, Lee Y. Characterization of natural dyes and traditional Korean silk fabric by surface analytical techniques. Materials 2013;6(5):2007.
[37] Liu J, Guo D, Zhou Y, Wu Z, Li W, Zhao F, et al. Identification of ancient textiles from Yingpan, Xinjiang, by multiple analytical techniques. J Archaeol Sci 2011;38(7):1763–70.
[38] Zhang X, Good I, Laursen R. Characterization of dyestuffs in ancient textiles from Xinjiang. J Archaeol Sci 2008;35(4):1095–103.
[39] Zhang X, Corrigan K, MacLaren B, Leveque M, Laursen R. Characterization of yellow dyes in nineteenth-century Chinese textiles. Stud Conserv 2007;52(3):211–20.
[40] Gibbs PJ, Seddon KR, Brovenko NM, Petrosyan YA, Barnard M. Analysis of ancient dyed Chinese papers by high-performance liquid chromatography. Anal Chem 1997;69(10):1965–9.
[41] Mouri C, Laursen R. Identification and partial characterization of C-glycosyl-flavone markers in Asian plant dyes using liquid chromatography–tandem mass spectrometry. J Chromatogr A 2011;1218(41):7325–30.
[42] Chen VJ, Smith GD, Holden A, Paydar N, Kiefer K. Chemical analysis of dyes on an Uzbek ceremonial coat: objective evidence for artifact dating and the chemistry of early synthetic dyes. Dyes Pigments 2016;131:320–32.
[43] Kramell AE, Wertmann P, Hosner D, Kluge R, Oehler F, Wunderlich C-H, et al. A multi-analytical techniques based approach to study the colorful clothes and accessories from mummies of Eastern Central Asia. J Archaeol Sci: Reports 2016;10:464–73.
[44] Feng Z. Textiles from Dunhuang in UK collections. Shanghai: Donghua University Press; 2007.
[45] Cave temples of Mogao at Dunhuang: art and history on the Silk Road. Los Angeles: The Getty Conservation Institute; 2015.
[46] Cave temples of Dunhuang: Buddhist art on China's Silk Road. Los Angeles: The Getty Conservation Institute; 2016.
[47] Stein A. Ruins of desert Cathay: personal narrative of explorations in Central Asia and Westernmost China. London: Macmillan & Co. Ltd; 1912.
[48] Feng Z. Textiles from Dunhuang in French collections. Shangai: China Textile University Press; 2011.
[49] Feng Z. Textiles from Dunhuang in Russian collections. Shangai: China Textile University Press; 2014.
[50] Tamburini D, Martin de Fonjaudran C, Verri G, Accorsi G, Acocella A, Zerbetto F, et al. New insights into the composition of Indian yellow and its use in a Rajasthani wall painting. Microchem J 2018;137(Supplement C):238–49.
[51] Dyer J, Tamburini D. An unusual pink colorant found on a Hellenistic oinochoe (to be updated). Dyes Pigments 2017. Forthcoming.
[52] Bansal V, Sharma A, Ghanshyam C, Singla ML. Rapid HPLC method for determination of vitamin C, phenolic acids, hydroxycinnamic acid, and flavonoids in seasonal samples of emblica officinalis juice. J Liq Chromatogr Relat Technol 2015;38(5):619–24.
[53] Zhao T, Sun Q, Marques M, Witcher M. Anticancer properties of Phyllanthus emblica (Indian gooseberry). Oxid Med Cell Longev 2015;2015:7.
[54] Yang B, Liu P. Composition and biological activities of hydrolyzable tannins of fruits of Phyllanthus emblica. J Agric Food Chem 2014;62(3):529–41.
[55] Kumar S, Singh A, Kumar B. Identification and characterization of phenolics and terpenoids from ethanolic extracts of Phyllanthus species by HPLC-ESI-QTOF-MS/MS. J Pharmaceut Anal 2017;7(4):214–22.
[56] Surowiec I, Szostek B, Trojanowicz M. HPLC-MS of anthraquinoids, flavonoids, and their degradation products in analysis of natural dyes in archeological objects. J Separ Sci 2007;30(13):2070–9.
[57] Nour V, Trandafir I, Cosmulescu S. HPLC determination of phenolic acids, flavonoids and juglone in walnut leaves. J Chromatogr Sci 2013;51(9):883–90.
[58] Liu J, Meng M, Li C, Huang X, Di D. Simultaneous determination of three diarylheptanoids and an α-tetralone derivative in the green walnut husks (Juglans regia L.) by high-performance liquid chromatography with photodiode array detector. J Chromatogr A 2008;1190(1):80–5.
[59] Abu-Reidah IM, Ali-Shtayeh MS, Jamous RM, Arráez-Román D, Segura-Carretero A. HPLC–DAD–ESI-MS/MS screening of bioactive components from Rhus coriaria L. (Sumac) fruits. Food Chem 2015;166:179–91.
[60] Regazzoni L, Arlandini E, Garzon D, Santagati NA, Beretta G, Maffei Facino R. A rapid profiling of gallotannins and flavonoids of the aqueous extract of Rhus coriaria L. by flow injection analysis with high-resolution mass spectrometry assisted with database searching. J Pharmaceut Biomed Anal 2013;72:202–7.
[61] Mouri C, Laursen R. Identification of anthraquinone markers for distinguishing Rubia species in madder-dyed textiles by HPLC. Microchim Acta 2012;179(1):105–13.
[62] Nirmal NP, Rajput MS, Prasad RGSV, Ahmad M. Brazilian from Caesalpinia sappan heartwood and its pharmacological activities: a review. Asian Pacific J Trop Med 2015;8(6):421–30.
[63] Cuong TD, Hung TM, Kim JC, Kim EH, Woo MH, Choi JS, et al. Phenolic compounds from Caesalpinia sappan heartwood and their anti-inflammatory activity. J Nat Prod 2012;75(12):2069–75.
[64] Peggie DA, Kirby J, Poulin J, Genuit W, Romanuka J, Wills DF, et al. Historical mystery solved: a multi-analytical approach to the identification of a key marker for the historical use of brazilwood (Caesalpinia spp.) in paintings and textiles. Anal Methods 2018;10(6):617–23.
[65] Surowiec I, Nowik W, Trojanowicz M. Identification of “insoluble” red dyewoods by high performance liquid chromatography–photodiode array detection (HPLC-PDA) fingerprinting. J Separ Sci 2004;27(3):209–16.
[66] Strych S, Trauner D. Biomimetic synthesis of Santalin A,B and Santarubin A,B, the major colorants of red sandalwood. Angew Chem Int Ed 2013;52(36):9509–12.
[67] Seshadri TR. Polyphenols of Pterocarpus and Dalbergia woods. Phytochemistry 1972;11(3):881–98.
[68] Liu R, Ye M, Guo H, Bi K, Guo Da. Liquid chromatography/electrospray ionization mass spectrometry for the characterization of twenty-three flavonoids in the extract of Dalbergia odorifera. Rapid Commun Mass Spectrom 2005;19(11):1557–65.
[69] Otłowska O, Ślebioda M, Kot-Wasik A, Karczewski J, Śliwka-Kaszyńska M. Chromatographic and spectroscopic identification and recognition of natural dyes, uncommon dyestuff components, and mordants: case study of a 16th century carpet with Chintamani motifs. Molecules 2018;23(2):339.
[70] Dyer J, Tamburini D, Sotiropoulou S. The identification of lac as a pigment in ancient Greek polychromy - the case of a Hellenistic oinochoe from Canosa di Puglia. Dyes Pigments 2018;149:122–32.
[71] Tamburini D, Dyer J, Bonaduce I. The characterisation of shellac resin by flow injection and liquid chromatography coupled with electrospray ionisation and mass spectrometry. Sci Rep 2017;7(1):14784.
[72] Gupta D, Bleakley B, Gupta RK. Dragon's blood: botany, chemistry and therapeutic uses. J Ethnopharmacol 2008;115(3):361–80.
[73] Baumer U, Dietemann P. Identification and differentiation of dragon's blood in works of art using gas chromatography/mass spectrometry. Anal Bioanal Chem 2010;397(3):1363–76.
[74] Arnone A, Nasini G, Vajna de Pava O, Merlini L. Constituents of dragon's blood. 5. Dracoflavans B1, B2, C1, C2, D1, and D2, new A-type deoxyproanthocyanidins. J Nat Prod 1997;60(10):971–5.
[75] Jianghao S, Long-ze L, Pei C. Study of the mass spectrometric behaviors of anthocyanins in negative ionization mode and its applications for characterization of anthocyanins and non-anthocyanin polyphenols. Rapid Commun Mass Spectrom 2012;26(9):1123–33.
[76] Sousa MM, Melo MJ, Parola AJ, Seixas de Melo JS, Catarino F, Pina F, et al. Flavylium chromophores as species markers for dragon's blood resins from Dracaena and Daemonorops trees. J Chromatogr A 2008;1209(1):153–61.
[77] Assimopoulou AN, Karapanagiotis I, Vasiliou A, Kokkini S, Papageorgiou VP. Analysis of alkannin derivatives from Alkanna species by high-performance liquid chromatography/photodiode array/mass spectrometry. Biomed Chromatogr 2006;20(12):1359–74.
[78] Han J, Weng X, Bi K. Antioxidants from a Chinese medicinal herb – Lithospermum erythrorhizon. Food Chem 2008;106(1):2–10.
[79] Wouters J, Grzywacz CM, Claro A. Markers for identification of faded safflower (Carthamus tinctorius L.) colorants by HPLC-PDA-MS - ancient fibres, pigments, paints and cosmetics derived from antique recipes. Stud Conserv 2010;55(3):186–203.
[80] Laursen R, Mouri C. Decomposition and analysis of carthamin in safflower-dyed textiles. e-Preservation Sci 2013;10:35–7.
[81] Clementi C, Basconi G, Pellegrino R, Romani A, Carthamus tinctorius L. A photophysical study of the main coloured species for artwork diagnostic purposes. Dyes Pigments 2014;103:127–37.
[82] Liang Z, Sham T, Yang G, Yi L, Chen H, Zhao Z. Profiling of secondary metabolites in tissues from Rheum palmatum L. using laser microdissection and liquid chromatography mass spectrometry. Anal Bioanal Chem 2013;405(12):4199–212.
[83] Ye M, Han J, Chen H, Zheng J, Guo D. Analysis of phenolic compounds in rhubarbs using liquid chromatography coupled with electrospray ionization mass spectrometry. J Am Soc Mass Spectrom 2007;18(1):82–91.
[84] Hongliang J, Árpád S, E JN, N TB, R GD. Analysis of curcuminoids by positive and negative electrospray ionization and tandem mass spectrometry. Rapid Commun Mass Spectrom 2006;20(6):1001–12.
[85] Jiang H, Timmermann BN, Gang DR. Use of liquid chromatography–electrospray ionization tandem mass spectrometry to identify diarylheptanoids in turmeric (Curcuma longa L.) rhizome. J Chromatogr A 2006;1111(1):21–31.
[86] Verma RS, Middha D. Analysis of saffron (Crocus sativus L. Stigma) components by LC–MS–MS. Chromatographia 2010;71(1):117–23.
[87] Carmona M, Sánchez AM, Ferreres F, Zalacain A, Tomás-Barberán F, Alonso GL. Identification of the flavonoid fraction in saffron spice by LC/DAD/MS/MS: comparative study of samples from different geographical origins. Food Chem 2007;100(2):445–50.
[88] Wang L, Liu S, Zhang X, Xing J, Liu Z, Song F. A strategy for identification and structural characterization of compounds from Gardenia jasminoides by integrating macroporous resin column chromatography and liquid chromatography-tandem mass spectrometry combined with ion-mobility spectrometry. J Chromatogr A 2016;1452:47–57.
[89] Zhou Y, Liu X, Yang J, Han Q-B, Song J-Z, Li S-L, et al. Analysis of caged xanthones from the resin of Garcinia hanburyi using ultra-performance liquid chromatography/electrospray ionization quadrupole time-of-flight tandem mass spectrometry. Anal Chim Acta 2008;629(1):104–18.
[90] Yang J, Ding L, Hu L, Jin S, Liu W, You Q, et al. Rapid characterization of caged xanthones in the resin of Garcinia hanburyi using multiple mass spectrometric scanning modes: the importance of biosynthetic knowledge based prediction. J Pharmaceut Biomed Anal 2012;60:71–9.
[91] Sasaki Y, Sasaki K. Analysis of protoberberines in historical textiles: determining the provenance of East Asian textiles by analysis of phellodendron. e-Preservation Sci 2013;10:83–9.
[92] Tian P-p, Zhang X-x, Wang H-p, Li P-l, Liu Y-x, Li S-j. Rapid analysis of components in Coptis chinensis franch by ultra-performance liquid chromatography with quadrupole time-of-flight mass spectrometry. Phcog Mag 2017;13(49):175–9.
[93] Mokhber-Dezfuli N, Saeidnia S, Gohari AR, Kurepaz-Mahmoodabadi M. Phytochemistry and pharmacology of Berberis species. Phcog Rev 2014;8(15):8–15.
[94] Xiaoyan X, Bohang S, Xueting Y, Guanying Z, Pengyi H, Huiyuan G. Identification and analysis of alkaloids in cortex Phellodendron amurense by high-performance

liquid chromatography with electrospray ionization mass spectrometry coupled with photodiode array detection. J Separ Sci 2014;37(13):1533–45.
[95] Valianou L, Stathopoulou K, Karapanagiotis I, Magiatis P, Pavlidou E, Skaltsounis A-L, et al. Phytochemical analysis of young fustic (Cotinus coggygria heartwood) and identification of isolated colourants in historical textiles. Anal Bioanal Chem 2009;394(3):871–82.
[96] Kite GC, Veitch NC, Boalch ME, Lewis GP, Leon CJ, Simmonds MSJ. Flavonol tetraglycosides from fruits of Styphnolobium japonicum (Leguminosae) and the authentication of Fructus Sophorae and Flos Sophorae. Phytochemistry 2009;70(6):785–94.
[97] Parveen I, Wilson T, Threadgill MD, Luyten J, Roberts RE, Robson PRH, et al. Screening for potential co-products in a Miscanthus sinensis mapping family by liquid chromatography with mass spectrometry detection. Phytochemistry 2014;105:186–96.
[98] Jie C, Chengle Y, Yan Q, Zhihong C, Daofeng C. Approach to the study of flavone di-C-glycosides by high performance liquid chromatography-tandem ion trap mass spectrometry and its application to characterization of flavonoid composition in Viola yedoensis. J Mass Spectrom 2014;49(10):1010–24.
[99] Hong Jun-Li, Zhou H-Y, Zhu J, Li L, Shu P, Qin X-Y, et al. Comparative analysis of major constituents in Viola yedoensis Makino and different species from the Genus Viola by high-performance liquid chromatography with chemometrics methods. J Med Plants Res 2011;5(21):5230–9.
[100] Jung M, Choi J, Chae H-S, Cho J, Kim Y-D, Htwe K, et al. Flavonoids from Symplocos racemosa. Molecules 2015;20(1):358.
[101] Li B, Abliz Z, Tang M, Fu G, Yu S. Rapid structural characterization of triterpenoid saponins in crude extract from Symplocos chinensis using liquid chromatography combined with electrospray ionization tandem mass spectrometry. J Chromatogr A 2006;1101(1):53–62.
[102] Liu J, Ji L, Chen L, Pei K, Zhao P, Zhou Y, et al. Identification of yellow dyes in two wall coverings from the Palace Museum: evidence for reconstitution of artifacts. Dyes Pigments 2018;153:137–43.
[103] Cuoco G, Mathe C, Vieillescazes C. Liquid chromatographic analysis of flavonol compounds in green fruits of three Rhamnus species used in Stil de grain. Microchem J 2014;115:130–7.
[104] Chen G, Li X, Saleri F, Guo M. Analysis of flavonoids in Rhamnus davurica and its antiproliferative activities. Molecules 2016;21(10):1275.
[105] Marques R, Sousa MM, Oliveira MC, Melo MJ. Characterization of weld (Reseda luteola L.) and spurge flax (Daphne gnidium L.) by high-performance liquid chromatography–diode array detection–mass spectrometry in Arraiolos historical textiles. J Chromatogr A 2009;1216(9):1395–402.
[106] March RE, Lewars EG, Stadey CJ, Miao X-S, Zhao X, Metcalfe CD. A comparison of flavonoid glycosides by electrospray tandem mass spectrometry. Int J Mass Spectrom 2006;248(1):61–85.
[107] Sathiamoorthy B, Gupta P, Kumar M, Chaturvedi AK, Shukla PK, Maurya R. New antifungal flavonoid glycoside from Vitex negundo. Bioorg Med Chem Lett 2007;17(1):239–42.
[108] Mouls L, Mazauric J-P, Sommerer N, Fulcrand H, Mazerolles G. Comprehensive study of condensed tannins by ESI mass spectrometry: average degree of polymerisation and polymer distribution determination from mass spectra. Anal Bioanal Chem 2011;400(2):613–23.